

**THE EFFECTS OF PEROXIDE TREATMENT ON COMPOSITES  
OF LINEAR LOW DENSITY POLYETHYLENE AND SHORT  
SISAL FIBRE**

by

Moipone Alice Mokoena

Submitted in accordance with the fulfilment of the degree

Master of Science ( M.Sc.)

in the

School of Chemical Sciences

Faculty of Natural and Applied Sciences

at the

University of the North (Qwaqwa Campus)

SUPERVISOR:

PROF. A.S. LUYT

CO-SUPERVISORS:

DR. I KRUPA, POLYMER INSTITUTE, SLOVAK ACADEMY OF SCIENCE

DR. V. DJOKOVIĆ, INSTITUTE OF NUCLEAR SCIENCES "VINČA", SERBIA

AND MONTENEGRO

## DECLARATION

I, Moipone Alice Mokoena, hereby declare that the research in this thesis is my own original work, and has not partly or in full been submitted to any other University in order to obtain a degree.

A handwritten signature in cursive script, appearing to read 'Mokoena', written over a horizontal line.

Mokoena, MA, Mrs

A handwritten signature in cursive script, appearing to read 'Luyt', written over a horizontal line.

Luyt, AS, Prof

## **DEDICATION**

**In loving memory of my late husband**

**Kgwarai John Mokoena**

## TABLE OF CONTENTS

	Page
Acknowledgements	i
Abstract	ii
List of abbreviations	iii
CHAPTER 1 (Introduction)	
1.1 Natural fibres as fillers	1
1.2 Polyethylene	6
1.3 Peroxide cross-linking and free radical grafting	7
1.4 Composites	9
1.5 Physical properties of composites	14
1.6 Chemical treatment of fibres	20
1.7 Objective of the study	23
CHAPTER 2 (Materials and methods)	
2.1 Materials	25
2.2 Composite preparation	25
2.3 Characterisation and analyses	26
2.3.1 Gel content	26
2.3.2 Fourier transform infrared (FTIR)	27
2.3.3 Water absorption	27
2.3.4 Dynamic mechanical analysis (DMA)	27
2.3.5 Differential scanning calorimetry (DSC)	28
2.3.6 Mechanical testing	28
2.3.7 Microscopy	29
CHAPTER 3 (Results and discussion)	
3.1 Characterisation of composites	30
3.1.1 Gel content	30
3.1.2 Fourier transform infrared (FTIR)	32

3.2	Water absorption	37
3.3	Thermal analysis	41
3.3.1	Dynamic mechanical analysis (DMA)	41
3.3.2	Differential scanning calorimetry (DSC)	42
3.4	Mechanical testing	50
3.4.1	Tensile strength	50
3.4.2	Stress relaxation	57
3.5	Microscopy	63
CHAPTER 4 (Conclusions)		65
REFERENCES		68

## ACKNOWLEDGEMENTS

I would like to extend my sincere gratitude to all who helped me through the course of the research, and preparation of this thesis. Special thanks goes to:

- My benefactors, NRF and the University of the North, for financial assistance
- Igor Krupa, for your inputs towards this research
- My colleagues and post-graduates, in the School of Chemical Sciences for helping in times of need. Your constant support and encouragement gave me the strength I needed
- Ebenezer group for all the motivation and spiritual nourishment
- My family for all the love and understanding, I would not make it without your support
- Fundis and company for all the efforts you put in this research
- Team from Budapest, Hungary for the valuable suggestion and skills that have been incorporated into this research Results and discussion
- My two sons, Majane and Moiloa, for your understanding and patience of the situation so hard for you to comprehend
- Freddy, for your unconditional care and support as well as the quality time you have put towards the success of this thesis
- Dr Djoković, for your patience in guiding while imparting knowledge and so much insight
- Prof Luyt, for your unwavering support and guidance, making every step of the way possible and successful

## ABSTRACT

In this work sisal fibre (*Agave sisalana*) was used as reinforcement in LLDPE-sisal fibre reinforced composites. In recent years there has been an increasing interest in finding new applications for sisal fibre as reinforcement in composites. The inherent problem that sisal fibre is hydrophilic in nature and thus absorbs a considerable amount of water, poses a threat towards achieving good interfacial adhesion with hydrophobic thermoplastic materials. Thus it was necessary to consider treatment of the composites. Dicumyl peroxide (DCP) was used for this purpose. The influence of sisal fibre and DCP content on the thermal, mechanical and visco-elastic properties of LLDPE-sisal fibre composites was investigated. Results show a significant decrease in water absorption for the DCP treated samples, changes in the polymer melting behaviour as a result of the presence of sisal as well as cross-linking/grafting in the presence of DCP, and significantly improved stress and strain at break, especially at low sisal contents. The presence of sisal increases the tensile modulus, but DCP treatment does not seem to have much influence on this property. Stress relaxation reduces with increasing sisal content, but again DCP treatment does not seem to have much influence. Although not proved beyond any doubt, there are indications that peroxide treatment, especially at high DCP content, causes grafting between LLDPE and sisal, as well as degradation of LLDPE.

## LIST OF ABBREVIATIONS

A	area (m <sup>2</sup> )
BP	benzoyl peroxide
CTDIC	cardanol derivative of toluene diisocyanate
DCP	dicumylperoxide
DSC	differential scanning calorimetry
DMA	dynamic mechanical analysis
EPM	ethylene propylene copolymer
$\Delta H_c$	enthalpy of crystallisation (J g <sup>-1</sup> )
$\Delta H_m$	enthalpy of melting (J g <sup>-1</sup> )
$\epsilon_b$	elongation at break
E	Young's modulus (MPa)
GF	glass fibre
H <sub>2</sub> SO <sub>4</sub>	sulphuric acid
HDPE	high-density polyethylene
LDPE	low-density polyethylene
LLDPE	linear low-density polyethylene
F	force (N)
FTIR	Fourier-transform infrared spectroscopy
KMnO <sub>4</sub>	potassium permanganate
MA	maleic anhydride
MaiPP	maleic anhydride isotactic polypropylene
MFI	melt flow index (g/10 min at a specified temperature)
m.p.	melting point (°C)
Mw	molecular weight
NaOH	sodium hydroxide
PE	polyethylene
PETF	polyester fibre
PP	polypropylene



$T_c$	crystallisation temperature ( $^{\circ}\text{C}$ )
$T_m$	melting temperature ( $^{\circ}\text{C}$ )
$T_{\text{max}}$	maximum temperature ( $^{\circ}\text{C}$ )
$T_{\text{o,m}}$	onset temperature of melting ( $^{\circ}\text{C}$ )
$T_{\text{p,m}}$	peak temperature of melting ( $^{\circ}\text{C}$ )
$T_g$	glass transition temperature ( $^{\circ}\text{C}$ )
TG	thermogravimetric analysis
$\sigma$	stress
UNSF	untreated sisal fibre
$W_{\text{abs}}$	water absorption (%)

# CHAPTER 1

## INTRODUCTION

### 1.1 Natural fibres as fillers

Fibre is a unit of matter characterised by flexibility, fineness and high ratio of length to thickness. It is useful that the fibre must be sufficiently uniform and its balance of properties and cost should be in accordance with the intended end use. Traditional fibre applications are in clothing and furnishing, but the range of fibre end-use is rapidly expanding, particularly in the industrial sector, for example composites and insulation. The wide range of materials classified as fibres include natural and synthetic, organic and inorganic products [1, 2]. Natural fibres are broadly classified into two types, namely:

- Carbohydrate, e.g. cellulose-based cotton and flax (first identified in Europe), and
- Proteinaceous e.g. keratotic animal furs (wool) and insect-based secretions (silk).

The class of polymers based on cellulose includes wood and most plant matter. Plant fibres are of interest because they probably represent the earliest textile materials. Another type is vegetable fibre, which is divided into long and multi-celled or short and single-celled. The focus of this text will be on the long and multi-celled fibre, which is further categorized into hard or soft according to the degree of stiffness and fibre fineness [3, 4].

Soft fibres are grouped into flax, hemp, jute and ramie, which are obtained from leaves of tropical plants, coir, which is derived from the coarse bristles enveloping the fruit of the coconut palm, and cotton and kapok, which are examples of the seed-hair and seedpod fibres, respectively. Hard fibres, on the other hand, are grouped into the leaf type e.g. sisal, and the palm type, e.g. coir or *cocos nucifera*. They are normally brown in colour, strong and flexible, and resistant to salt water. For this reason they are used for marine applications and heavy domestic work [5, 6]

Although natural vegetable fibre characteristics can vary somewhat with the environmental conditions under which the plants grow, chemically they consist of mainly cellulose (Figure 1.1), including hemicelluloses, moisture, lignin and pectin, with residual amounts of ash and other organic material. Cellulose is a polysaccharide made up of  $\beta$ -D(+)-glucose residues joined in linear chains having the structure shown in Figure 1.1 [3, 7].

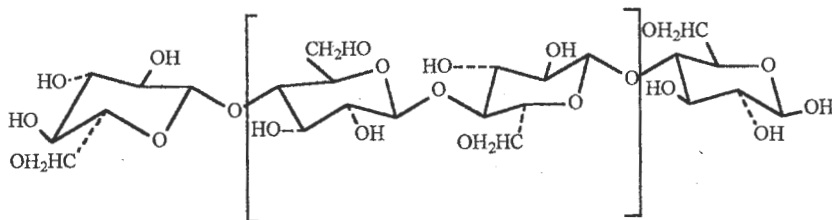


**Figure 1.1** The molecular structure of cellulose, based on  $\alpha$ -D-glucose monomer units with  $\beta$ -1-4-glycosidic links

With its hydroxyl groups, cellulose has the opportunity of forming many hydrogen bonds. The resulting high intermolecular forces, plus the regular structure of the polymer, results in it having an unusually high degree of crystallinity. The crystalline melting point is far above its decomposition temperature. The solubility of the polymer is very low, and it is doubtful that solution ever takes place unless a chemical derivative is formed. Cellulose does swell, however, in hydrogen-bonding solvents, including water. The swelling is, of course, restricted to the amorphous regions of the fibre that is composed predominantly of cellulose of high  $M_w$ , typically  $6 \times 10^5$  and larger, consisting of long chains of D-glucose units joined by  $\beta$ -1,4-glycosidic links [3, 7].

Edwards *et al.* [7] studied the application of FT-Raman microscopy of seven plant fibres, which have cellulose contents ranging from 64 to 91 %, water from 0 to 12 %, and lignins/pectins from 0 to 25 %. Their studies on natural fibres were done without any pre-treatment, either of a chemical or mechanical nature. This minimises the introduction of changes in the cellulose structure through processing or storage. Degradation of cellulose would be expected to produce first a decrease in the band at  $1096 \text{ cm}^{-1}$  through fission of the  $\nu(\text{COC})$  glycosidic linkages, and an increase in the band profile around  $2900 \text{ cm}^{-1}$  due to new  $\nu(\text{CH})$  modes arising from the decomposition products. This could be a useful parameter for study of ancient fibres.

Khalil [9] embarked on a study for determining the effect of acetylation on the interfacial shear strength between plant fibre and various matrices. They observed the following three major changes as a result of acetylation:

- An increase in the carbonyl ( $\text{C}=\text{O}$ ) stretching region ( $1750 \text{ cm}^{-1}$ ) [1744 for coir],
- An increase on the carbon-hydrogen ( $\text{C}-\text{H}$ ) bond stretching region ( $1375 \text{ cm}^{-1}$ ) [1381 for coir] and
- An increase in the carbon-hydrogen ( $\text{C}-\text{H}$ ) stretch, around  $1238 \text{ cm}^{-1}$ .

The peak regions varied according to the type of fibre used. The absorption at  $3400 \text{ cm}^{-1}$  (for an unmodified sample) is due to both the hydroxyl group and absorbed moisture, through the



followed by brushing and fibres are then graded, pressed in a Bios, which is a high density press, and are ready for transporting and twining in the making up of ropes.

**Figure 1.3** Cutting of sisal plant leaves after 4 years

Though sisal fibre is one of the most widely used natural fibres, a large quantity of this economic and renewable resource is still under-utilized [3]. At present, sisal fibre is mainly used as ropes (Figure 1.4) for the marine and agricultural industry. Other applications of sisal fibre include twines, cords, upholstery, padding and mat making, fishing nets, fancy articles such as purses, wall hangings, and tablemats. Recent manufacture of corrugated roofing panels, that are strong and



cheap with good fire resistance, proved to be potential applications [3, 9]. Sisal fibre is chosen as organic filler on account of its excellent mechanical properties, for instance, its low cost, low density, high specific strength (in the range 38-55 MPa) and modulus (between 3600-4800 MPa), low health risk, easy availability and renewability.

**Figure 1.4** Rope made from sisal fibre

During the past number of years the identification of new application areas for this economical material has become a vital task. The use of sisal fibre as a reinforcement in composites has raised great interest and expectations amongst materials scientists and engineers [9]. The major studies carried out during this period can be broadly divided, as stipulated by Li *et al.* [5], into the following topics:

- ❖ Properties of sisal fibre: Mechanical, thermal and dielectric properties of sisal fibre have been studied in detail. FTIR, TG, DSC, and DMA have been used to determine the characteristics of sisal fibre and provide theoretical support for processing and application of this fibre.
- ❖ Interface properties between sisal and its matrix: the main purpose here is to modify the fibre surface structure by using chemical and thermal treatment methods in order to enhance the bond strength between fibre and matrix and reduce water absorption of sisal fibre.

formation of hydrogen bonding between the groups and water. Acetylation results in an increase of the hydrophobicity of the fibres, due to the introduction of acetyl groups through the substitution of the OH group of the fibre. It can therefore be postulated that the degree of moisture adsorption is accordingly reduced.



Sisal fibre is one of the most widely used natural fibres and is very easily cultivated. Sisal has short renewal times and grows wild in the hedges of fields and railway tracks. Nearly 4.5 million tons of sisal fibre are produced every year throughout the world. Though native to tropical and sub-tropical North and South America, sisal is now widely grown in tropical countries of Africa, the West Indies and the Far East [3, 5].

**Figure 1.2** Sisal plant, called *Agave sisalana*

Sisal fibre is a hard fibre extracted from the leaves of the sisal plant (*Agave sisalana*), commonly known as aloe in South Africa (Figure 1.2). The sisal leaf contains three types of fibre, namely mechanical, ribbon and xylem. The mechanical fibres are mostly extracted from the periphery of the leaf, have a roughly thickened horseshoe shape, and rarely divide during the extraction process. They are commercially the most useful for sisal fibre. Ribbon fibres occur in association with conducting tissues in the median line of the leaf. The ribbon fibres are the longest fibres and, compared to mechanical fibres, can be easily split longitudinally during processing. Xylem fibres, on the other hand, have an irregular shape, occur opposite the ribbon fibres through the connection of vascular bundles, are composed of thin-walled cells, and are easily broken up and lost during the extraction process. After extraction, the fibres are washed thoroughly in plenty of clean water to remove the surplus wastes such as chlorophyll, leaf juices and adhesive solids [5].

The processing method for extracting sisal fibres was given by the National Sisal Marketing Committee in Pietermaritzburg, South Africa (Figure 1.3). The method includes planting on the 2000 hectares Cango farm, which is situated in Zululand, about 270 km North of Durban. Weeding is by hand and plants are cut after 4 years. Cutting of plants normally takes 16 to 20 months. This is followed by bundling and transporting to a sisal mill. Plants are put in a decorticator, then under a double squeezer to remove almost 50 % water from the decorticated plants. The fibers are then put in a machine drier, which utilizes hot air to reduce moisture content to 2 %. Drying is then

- ❖ Properties of sisal fibre-reinforced composites: The matrices used in sisal-reinforced composites include thermoplastics (polyethylene, polypropylene, polystyrene, PVC, etc.), thermosets, rubber, gypsum and cement.
- ❖ Sisal/glass reinforced hybrid composites: To take advantage of both sisal and glass fibre, they have been added jointly to the matrix so that an optimal, superior but economical composite can be obtained. The hybrid effect of sisal/glass fibres on the mechanical properties have been studied and explained [5].

The strength and stiffness of plant fibres depend on the cellulose content and the spiral angle, which the bands of microfibrils in the inner secondary cell wall make with the fibre axis. The structure and properties of natural fibres depend on their source and age. The tensile properties of sisal fibre are not uniform along its length. The root or lower part has a low tensile strength and modulus, but high fracture strain. The fibre becomes stronger and stiffer at midspan and the tip has moderate properties. Studies show the effects of fibre diameter and test speed on the tensile strength, initial modulus and percent elongation at break of sisal fibres. No significant variation of mechanical properties with change in fibre diameter was observed. However, the tensile strength and percent elongation at break decrease, while Young's modulus increases with fibre length. With increasing speed of testing, Young's modulus and tensile strength both increase, while elongation does not show any significant variation. At higher speeds, about  $500 \text{ mm min}^{-1}$ , the tensile strength decreases sharply [5].

Simple esterification and etherification reactions were applied to stem-exploded flax with the aim of changing the surface properties through modification of fibre surface chemistry by Baiardo *et al* [10]. Native and chemically modified cellulose fibres were characterized in terms of thermal stability, surface chemistry, morphology, and crystal structure. Independent of the substituent nature, chemically modified fibres exhibited a thermal stability comparable to that of native cellulose. From the FTIR spectra, they observed that the substitution reaction involved only a small fraction of the cellulose hydroxyls. There was no change in the native crystalline structure of cellulose fibres during chemical modification, except in the case where ether substitution was carried out in a water-isopropanol medium. This was shown by a substantial consistency of the intensity of the  $\text{-OH}$  stretching absorption band ( $3380 \text{ cm}^{-1}$ ) of cellulose after both esterification reactions.

## 1.2 Polyethylene

Polyethylene is an example of a semi-crystalline polymer, which has one of the simplest molecular structures  $[-\text{CH}_2-\text{CH}_2-]_n$  and is at present the largest tonnage plastic material used in electrical insulation. Polyethylene normally forms tough, flexible plastic materials with a large variety of uses, and is the world's fastest growing polymer family. There are a number of good reasons for this, one of which is cost-performance [5]. Most members of this family are easy to fabricate and have low cost, and there is a wide difference in their properties.

Low-density polyethylene, LDPE, has good mechanical properties and is often used in industry. It is a partially (40 – 60 %) crystalline solid that melts at about 110-115 °C, and has a density in the range of 0.91 – 0.94 g.cm<sup>-3</sup> [1, 11]. It has high impact strength, low brittleness temperature (which makes it flexible), film transparency and outstanding electrical properties. The physical properties of LDPE are functions of three independent structural variables: molecular weight, short chain branching and long chain branching. Short chain branching is assumed to affect morphological and solid state properties, while long chain branching is mostly manifested in viscoelastic properties. Short chain branching has a predominant effect on the degree of crystallinity and therefore on the density of LDPE. LDPE is less crystalline than HDPE, and is flexible and clear with moderate toughness [1, 11, 12].

High-density polyethylenes, HDPE, are highly crystalline polymers used in molding and film applications, for example milk jugs. They are less flexible than other polyethylenes. They have higher melting points in the range 130-138 °C, and they have densities around 0.941-0.954 g cm<sup>-3</sup> [1, 12].

Linear low-density polyethylenes, LLDPE, are copolymers of ethylene with modest amounts of butene, hexene, or octene, which are alpha-olefins. They are linear, but have a significant number of short hydrocarbon branches and usually have a melt flow index (MFI) of 3.5 g /10 min, and a density of about 0.938 g.cm<sup>-3</sup> [1, 11]. The presence of short carbon chains brings about reduced structural regularity and consequently crystallization. LLDPE have good mechanical properties and are often used in industry. Grocery bags, heavy-duty slapping sacks, agricultural films, pipes, and liners for consumer's landfills and waste ponds are only a few examples. The linearity provides strength, while the branching provides toughness. Grades are available for films and for molding. Films typically show good toughness and some grades are suitable for fibres. In general, the polymer has similar properties to LDPE, but shows better strength properties in films, which is its

preferable area of use. The only disadvantage is that LLDPE is less pseudoplastic than LDPE and so its melt viscosity is higher during processing. Studies also show that LLDPE may phase separate in the melt. LLDPE represents a relatively new class of materials that entered the commercial market in the early 1980s. These materials were developed in order to produce a polyethylene with short chain branches, without any long chain branches [1, 11, 12].

Polyethylene samples are chemically very inert. They do not dissolve in any solvents at room temperature, but are swelled at higher temperatures. They have good resistance to acids and alkalis. They were found to be unaffected by strong acids like  $H_2SO_4$  and HCL at 100 °C. However, concentrated nitric acid chars it. They are often used in containers for acids, including hydrofluoric acid. Several studies [11, 12] show that they age on exposure to light and oxygen, with loss of strength, elongation and tear resistance. The polymers also undergo some cross-linking when heated or worked at elevated temperatures.

Studies on the thermal expansion behaviour of oriented polyethylene were conducted over a range of different temperatures, and Orchard *et al.* [13] made some remarkable observations. The values for the thermal expansion coefficient in the orientation direction are negative and of a greater magnitude than the c-axis expansion for the crystal, which is approached at -50 °C. These have been supported by modulus measurements over the same range and by measurements of the shrinkage force obtained when samples are immersed in an oil bath at the processing temperature. They showed that the irregular negative expansion coefficient measured in highly oriented polyethylene samples are not simply due to a negative expansion coefficient of the crystalline regions, but can be attributed to an internal stress in the sample, which causes a changing strain as the sample modulus, and the internal stress, though to a lesser extent, vary with temperature.

### **1.3. Peroxide cross-linking and free radical grafting**

Often grafting is a desired reaction for selected monomers onto polymer chains. This may occur when a microradical reacts with the double bond of the vinyl monomer, forming a branched macroradical. The grafts onto the polymer chain are responsible for property improvement. Free radical initiators are sources of free radicals necessary for initiating a free radical grafting process. Those used to initiate a grafting reaction can be organic peroxides. Free radicals may also be generated by pure thermal and mechanical means. But under normal grafting conditions in solutions or in the melt, free radicals formed by thermo-mechanical means under ambient atmosphere are at concentrations too low to bring about grafting to a desired extent. The most



useful source is organic peroxides (ROOR'), which are often added in small amounts to the grafting system. Dicumyl peroxide (DCP) is an example of this family [1, 14].

Efforts to modify polyolefins by free radical grafting of polar monomers, have been in process since the 1960s [1, 12]. One of the most important challenges facing melt free radical grafting was to obtain a sufficient amount of grafted initiator onto the polymer backbone, while maintaining the mechanical properties and thus the molecular weight of the original polymer. Interesting studies were performed on the melt grafting of maleic anhydride (MA) onto an isotactic polypropylene (PP) in a Brabender batch mixer, using benzoyl peroxide (BP) or dicumyl peroxide (DCP) as free radical generators [1, 12]. Despite a notable difference in the rates of decomposition, these two peroxides give virtually the same grafting yields at 185 °C. It is also noted that temperature has a deteriorating effect on the melt free radical grafting, while the rate of grafting also plays an important role.

Despite intensive scientific research and industrial practice, for over 30 years melt free radical grafting of monomers onto polymer chains has become controllable only recently. In the past, the main concern in melt free radical grafting was a lack of efficient methods to achieve two opposing requirements: to attain (i) a sufficient yield with (ii) a minimum change in molecular architecture of the original polymer substrates. Very often attainment of a sufficient grafting yield was accomplished by a drastic change in molecular architecture and consequently in physical, rheological as well as mechanical properties of the original polymer substrates. For example, a large amount of peroxide had to be added to raise the MA grafting yield onto polyethylene or polypropylene. This however, resulted in the formation of cross-links with PE or molecular degradation of the PP [1, 12].

Incorporation of relatively stable peroxides, such as dicumyl peroxide and di-*t*-butyl peroxide, provides a chemical means of cross-linking polyethylene. Chemically cross-linked polyethylenes are used in the wire and cable industry and are of interest for pipe, hose and moulded articles. Various authors [1, 11, 15] outline investigations that were performed on peroxide cross-linking of HDPE and LDPE using DCP. Peroxides suitable for cross-linking should slowly decompose at the processing temperature used for their incorporation into the polyolefin melt. They found that for cable applications DCP was more suitable for LDPE than for the higher melting point HDPE. In hot water pipe applications, HDPE had been of main interest. There were improvements in creep, impact and chemical resistance after cross-linking. Pipes with longer lives for hot water, and for the transport of chemically aggressive media, were obtained. However, higher temperatures had to be

used, owing to the higher melting point of HDPE. Consequently this has complicated the utilisation of peroxide in the pipe area. It has however instilled interest in other spheres of polymer engineering such as modification of PE-fibre composites.

Over the years cross-linking had become a broadly used method for the modification of polymer properties. This process involves the formation of three-dimensional structures (gels) that cause substantial changes in material properties. Different procedures may be used for the initiation of polyolefin cross-linking. One is based on macro-radical formation via thermal decomposition of organic peroxides. The molecular weight of polymers increases during cross-linking, and this is directly interrelated with the change of properties of the polymer connected with the sample deformability. The cross-linking leads to an increase in the viscosity of the polymer melt, increased tensile strength, improvement of creep properties and in an increase in the resistance to environmental stress cracking. It stabilises the natural molecular network and every system is potentially elastically operative and can contribute to the stress in tensile experiments.

Cross-linking reduces the polyolefin's crystallinity [13, 16]. Krupa and Luyt [17] observed a decrease in the degree of crystallinity of LLDPE with an increase in DCP content. Cross-links play the role of defect centres, which impede the folding of macromolecular chains. The size of the lamellar crystals is consequently reduced.

#### 1.4 Composites

There is no widely accepted definition of what a composite material is, but an Oxford Complete Word-Finder explains it as a synthetic built made up of distinct parts or constituents. The Dictionary of Polymer Science explains it as a solid material which consists of two or more simple materials with at least about 5 % of each phase being present in intimate mixture, and in which the individual components retain their separate identities [3]. At the macro-structural level, a glass matrix reinforced plastic in which the naked eye distinctly recognizes the glass fibre, is considered a composite material. According to Smith [14] a composite material is a material system composed of a mixture or combination of two or more micro- or macro-constituents that differ in form and chemical composition, and which are essentially insoluble in each other.

The term *composites* is generally applied to fibre-reinforced engineering structural materials, in which the fibres are continuous or long enough so that they can be oriented to produce enhanced strength properties in one direction [10]. The engineering importance of a composite material is

that two or more distinctly different materials combine together to form a material, which possesses properties that are superior, or more important in some other manner, to the properties of the individual components. Studies show that sisal fibre is a promising reinforcement for use in composites on account of its low cost, low-density, high specific strength and modulus, low health risk, easy availability, and renew-ability.

Filled polymers are the simplest type of composite polymeric materials, which consist of a matrix polymer as a continuous phase and generally inorganic filler dispersed in the matrix. Fillers are added to modify various properties such as mechanical and electrical properties, or simply as extenders for lowering the price/volume ratio of the material [18]. Fibre-reinforced composites are a very intensively studied area, which proved to have big practical importance worldwide. The reason for this is that most organic fillers are natural components, for example sisal, flax, chopped grass, and wooden flour. They are mostly renewable, very cheap products and often produce even cheaper composites if they are mixed with polymers. The composites with organic fillers are also reported to be biodegradable, which is the most desirable behaviour, and implies that it is safe to work with them, as they have no health hazards [5, 8].

Fillers are frequently added to polymers to lower their price. Usually such fillers are finely ground inorganic materials, such as chalk, silica and clay. However, natural fibres can behave as fillers if finely ground. As a result of the presence of filler, the mechanical properties of the material are changed. Impact and tensile strengths are usually decreased while hardness and stiffness are increased. If the polymer molecules are adsorbed on the filler surface their mobility is restricted. As a result the glass transition of the adsorbed polymer will increase.

Studies had shown that research interest has changed from the fibre itself to sisal-reinforced composites and hybrid composites. Owing to the increased use of thermoplastics, studies of sisal-reinforced thermoplastics, as well as that of the interface between sisal and the matrix, have become increasingly important. Most studies show that interfaces play an important role in the physical and mechanical properties of composites. The hydroxyl groups, which occur throughout the structure of natural fibres, make them hydrophilic, but many polymer matrices are hydrophobic so that sisal-polymer composites have poor interfaces. Hydrophilic sisal fibres will also absorb a large amount of water in the composite, leading to failure by delamination. It is therefore important to consider surface treatment and the resultant effects on the physical and mechanical properties of different fibre-matrix composite systems [19].

The free plastic shrinkage of composites reinforced with natural sisal fibre has been studied using a factorial design of experiments. This technique produces great savings in time, resources, and investigation costs and leads to a mathematical model the results of which presented good correlation with the experimental ones in the range of factors investigated. Low-volume sisal and polypropylene fibre were found to be extremely effective in reducing free plastic shrinkage, in retarding the first crack appearance, and in controlling crack development. These happen because at early age the elastic modulus of these fibres is still higher than that of the cementitious matrix [20].

The original purpose of adding mineral fillers to polymers was that of cost reduction. However, in recent years fillers have come to play an increasingly functional role. Addition of natural fillers was a common practise for improving cost/performance ratios of polyolefins, with particular reference to the increase of stiffness and temperature resistance, and to the reduction of creep, shrinkage, warpage, and thermal expansion. In general, it can be stated that the mechanical properties, and in particular impact strength and toughness, can be drastically varied, depending on matrix characteristics, type and content of filler, and the adhesion between filler and matrix. For a fundamental understanding of the material properties as well as for optimised processing, the melting behaviour and the crystallinity of a matrix in a filled system is of importance [5, 21]. During the past 80 years a number of materials, using the reinforcing properties of wood cellulose, have found major markets. Recent attention has been given to them as fillers or reinforcements in thermoplastics and elastomers. Most cellulosic composites derive their existence from their comparatively low material cost and the filling rather than reinforcing properties of cellulose. However, cellulose chains have a potential stiffness much higher than glass and in the same range as superstiff aramid fibers [22].

The structure-property relationship of wood flake-high-density polyethylene (HDPE) composites was studied by Balasuriya *et al.* [22] in relation to the matrix agent's melt flow behaviour and processing technique. They optimised flake distribution and flake wetting to obtain acceptable mechanical properties in these composites using two techniques, namely twin-screw compounding and mechanical blending. They observed from the microstructure of the composites that the twin-screw compounded composites, based on medium melt flow index (MMFI) HDPE, always achieved better flake wetting and distribution, and therefore had higher mechanical properties, than those mechanically blended composites or twin-screw compounded composites with low MFI (LMFI) HDPE. For 50:50 wt % composites the overall flake wetting, depending on processing technique and matrix flow behaviour, is ranked as compounded MMFI > compounded LMFI > blended

MMFI > blended LMFI. The uniformity of flake distribution of the composites follows a different pattern: compounded MMFI > blended MMFI > compounded LMFI > blended LMFI. They found that the medium MFI HDPE penetrates into lumens of wood fibres in wood flakes.

Privalko *et al.* [23] described in their paper that the melting temperature,  $T_m$ , of HDPE is composition independent, and fluctuates around the mean value of  $T_m = 402 \pm 1,5$  K. This result implies that the mean dimensions of lamellar HDPE crystals in the composites are not appreciably affected by the filler particles of kaolin. In contrast, the values of the melting enthalpies,  $\Delta H_m$ , of the HDPE crystals in composites estimated by a linear extrapolation of the best fits of the experimental data down to  $W = 0$ , are higher than the measured values of  $\Delta H_m$  for the neat polyethylenes. In quantitative terms, the degree of crystallinity of the HDPE matrix increased with respect to the changing amount of filler. This was explained in terms of the nucleating effect of the kaolin particles on the melt crystallization of HDPE, which promotes higher crystallinities of the HDPE matrix.

In composite materials, the interfacial properties are also important, in addition to the individual phases of the fibre and the matrix. Dynamic mechanical measurements over wide temperature or frequency ranges are useful in the understanding of the viscoelastic behaviour and provide valuable insights into the relationship between structure, morphology, and application properties of polymeric and composite materials. Amash and Zugenmaier [24] investigated the thermal behaviour and dynamic mechanical properties of isotactic polypropylene (PP) and reactor blend PP-ethylene propylene copolymer (EPM), reinforced by different amounts of short glass fibre (GF) or polyester fibres (PETF) by DSC and dynamic mechanical thermoanalysis (DMTA). Their DSC results showed an increase in the crystallization temperature of PP in the presence of fibres, but indicated no change in its percentage of crystallinity. They observed an increase in the stiffness and a decrease in damping with increasing GF content from DMTA measurements. The positions of the primary relaxations of the respective composites do not show any change, but a significant broadening of the alpha-relaxation in the crystalline phase is observed due to the induced reinforcement and interfacial interactions. They also discovered that the addition of PETF to PP enhanced its damping values at low temperatures and promoted the alpha-transition, while with an increase in GF content Young's modulus increased and  $\tan \delta$  decreased in a regular manner [24, 25].

The use of fibre-reinforced composites has grown dramatically in the last few years. In many applications these materials may come into contact with water (vapour or liquid) as well as organic

solvents. Consequently, it is very important to understand how the permeation properties of the polymers used can affect the mechanical properties of the composites. Water permeation, for instance, can lead to problems of dimensional change due to swelling of the matrix, as well as to chemical alternations within the composites [14].

Raghavan and Emekalam [26] characterized starch-PE and starch-PE-poly(lactic acid) composites using FTIR analyses. They concluded that the quantity of water passing through the porous and hydrolysed composites depended on the thickness of the film. Upon acid exposure, the composites were found to be poorly hydrolysable, and bands that are attributed to the starch content in the composite, decrease with time of acid exposure. This indicates that acid hydrolysis of starch involves the cleavage of glycosidic bonds through the addition of water. The starch was preferentially removed as hydrolysis progressed, leaving behind the PE matrix not significantly changed. An extensive degradation of starch occurs in the film, which gives rise to a gradual disappearance of the C-O band. During the same period, the C=O band in the range 1700 to 1760  $\text{cm}^{-1}$  was not observed to decrease significantly.

Natural fibres, when used as reinforcement, compete with technical fibres, such as glass fibre or carbon fibres. The advantages of technical fibres are good mechanical properties, which vary only little, but with the disadvantage that they are difficult to recycle. The mechanical properties of composites are influenced mainly by the adhesion between matrix and fibres. Pre-treating the fibres can change the adhesion properties. Moisture repellence, resistance to environmental effects, and mechanical properties are improved by surface treatment of fibres. Various applications of natural fibres as reinforcement in plastics have proved encouraging. Several natural fibre composites reach the mechanical properties of glass fibre composites, and they are already applied, for example, in automobile and furniture industries. However, the development of processing and modification methods is not finished. Further improvements can be expected, so that it might become possible to substitute technical fibres in composites quite generally. Natural fibres are renewable raw materials and their composites are recyclable [3].

Several researchers have reported on the improvement of thermal conductivities of polymers by fillers, one of which is the analysis and presentation by Kalaprasad *et al.* [27] on the thermal conductivity and thermal diffusivity of sisal-reinforced, glass-reinforced and sisal glass hybrid fibre-reinforced polyethylene composites. They showed that the thermal conductivity increased with temperature, and levelled off afterwards. It was also observed that the thermal conductivity of polyethylene and sisal reinforced polyethylene composites are almost similar, because the

orientation of sisal in sisal-reinforced polyethylene is perpendicular to the applied thermal flux. The variation of thermal diffusivity, on the other hand, is opposite to that of thermal conductivity.

### 1.5 Physical properties of composites

Cellulose, added to thermoplastics, affects many of their physical properties. For instance, the presence of microcrystalline cellulose fibres shifts the glass transition temperature, and causes trans-crystallization in crystalline polymers. Due to the hydrophilic nature of cellulose fibres, the water absorption properties of the resulting composites are increased. Zang and Saphieha [28] investigated, by using DSC, the thermal properties of composites based on natural cellulose fibre and LLDPE. Their results showed an endothermic peak, which consists of two main components corresponding to polymer fusion and the dehydration of cellulose. For the LLDPE containing high concentrations of cellulose, or following immersion in water, a shoulder at temperatures above the melting peak was observed, which is due to the desorption of water from cellulose. It has been shown that the composition, degree of crystallinity, and water content of the composite can be easily determined from the DSC curves. A simple method to distinguish between the energy of dehydration and the enthalpy of fusion of the composites was proposed. At low cellulose content, the effect of the crystallinity change is predominant, and consequently the apparent enthalpy of fusion increases. With increasing cellulose content the effect of the water desorption process becomes dominant. The study showed that the apparent enthalpy of fusion is directly proportional to the LLDPE content, thus demonstrating the correspondence to the heat of fusion of the polymer. The linear relationship between enthalpy of fusion of composites and LLDPE content, however, implies that cellulose fibres have little effect on the overall crystallinity of the LLDPE. Again, the apparent energy of dehydration is close to the heat of evaporation of water, suggesting that only free water is being removed from the composites and that the diffusion energy of the water vapour through molten polyethylene is negligibly small.

Mishra *et al.* [29], in their recent work, used banana, hemp and sisal fibres as fillers in novolac resin. These fibres were treated with maleic anhydride (MA) and their effect on the swelling and mechanical properties of plant fibre polymer composites was assessed. Higher absorption of steam and water was observed in untreated fibre composites. The treated and untreated hemp, banana and sisal fibre composites showed an increase in steam absorption with an increase in fibre content. However, the absorption of steam decreases beyond 45 % of fibre amount in all MA treated and untreated sisal fibre composites. The steady increase in absorption of steam in untreated hemp and banana fibre composites is due to the availability of the free -OH groups. However, the

esterification of the –OH group by maleic anhydride minimizes the capability of the cellulose fibres to absorb steam. Sisal fibre composites show declining water absorption, but the water absorption increases sharply in composites with higher fibre content. The order of water absorption is hemp > banana > sisal. It was further observed from the results that untreated fibre composites show higher water absorption than treated fibre composites.

The degradation and moisture uptake of sago-starch-filled LLDPE composites had been studied by Denjaji *et al.* [30]. The study was based on the fact that plastic waste proves to be a serious environmental problem, and that PE, being the largest volume plastic used in packaging, is the worst offender and is highly resistant to biodegradation. They discovered that exposure of the composites to weathering resulted in massive deterioration, embrittlement and dimensional changes. The drop in mechanical properties of the composites also increased with time of burial for the first four months, and decreased gradually thereafter. Moisture uptake increased with increased starch content and immersion time. The time taken for the composites to equilibrate was independent of how the composites were exposed to water. The mechanical properties of the composites also dropped with increasing moisture uptake. The tensile strength and elongation at break decreased with time of immersion and starch content, due to the presence of moisture at the LLDPE-starch interface, which weakens the already weak interfacial adhesion. Their figures also showed that the reduction in tensile properties is directly related to immersion time - the longer the immersion period the greater the loss in tensile properties. The ability of these composites to absorb moisture not only reduces their mechanical properties, but also renders them susceptible to fungal attack, thus limiting their use.

The mechanical behaviour of polymers is strongly dependent upon the temperature and rate of testing. In general they display aspects of both elasticity and viscosity and so have been termed viscoelastic. For example, Young's modulus of a polymer depends upon the length of time the material is loaded. The phenomenon of creep, which is the increase in strain with time at constant applied stress, and stress relaxation, which is the decrease in stress at constant strain, are examples of time-dependent properties. The toughness of polymers depends upon material variables, such as polymer structure and orientation, and external variables, such as environment rate and temperature. The dependence is analogous to that of strength. For example, the fracture energy of an elastomer, such as styrene-butadiene rubber, is found to depend upon both testing rate and temperature. Fracture energy increases with both increasing rate and decreasing temperature. Furthermore, in rubber-toughened systems, the toughness of the polymer generally increases with an increase in



volume fraction of rubber particles, although when the particles have a complex structure the morphology of the particles can also have an effect upon the toughening efficiency [1, 10].

Polymers are prone to premature failure during cyclic deformation or fatigue loading, whereby cracks propagate at lower stresses than during monotonic loading. The process of fatigue takes place by the accumulation of damage at the crack tip. Extensive studies have taken place to characterize the fatigue behaviour of many types of polymers [1,14]. One other area where problems are often encountered with polymer toughness is in high strain rate deformation or impact. Material which are apparently tough at low rates of testing, become quite brittle when subjected to impact loading. Significant advances have been made in recent years, both in producing impact-resistant polymers and in understanding what is measured during an impact test.

A variety of models have been employed to explain the viscoelastic behaviour of a polymeric material. The Maxwell unit, consisting of a spring and dashpot in series, and the Kelvin (or Voigt) unit, consisting of a spring and dashpot in parallel, are the simplest of these models. The two models lead to analogous equations and have similar limitations. The stress-strain behaviour for the spring in the Maxwell model, assuming only small deformations are involved, is described as linear elastic. One of the applications of the Maxwell model has been in the treatment of stress relaxation. However, this model has serious deficiencies. For the case of a constant stress experiment it predicts Newtonian flow, which is not generally observed, the experimental behaviour being considerably more complex. Secondly, a simple exponential does not normally describe stress relaxation. Thirdly, the model is not able to adequately describe the dynamic-mechanical response of a polymer subjected to a sinusoidally applied stress [1, 10].

The general difficulty that may be encountered when using the two models is that the Maxwell model cannot account for a retarded response, and the Voigt model gives a retarded elastic response, but does not describe stress relaxation, and both models are characterized by a single relaxation time. A spectrum of relaxation times would be preferred for better description. These limitations brought fourth challenges for scientists to come up with models that will explain various properties (mechanical, electrical, etc.) of composite materials [10, 31, 32].

Among the mechanical properties yield stress of composites has primary importance, giving information on the maximum allowed load without considerable plastic deformation. The yield stress of composites depends, however, in a very complex way on the microstructure, since the load transfer between the phases and also the concentration is determined by structural factors, such as

the form and size distribution of the filler, its spatial distribution in the matrix, thickness of the interface, etc. In the case of zero adhesion between the filler particles and the continuous polymer phase, there is no load transfer to the filler and the matrix carries the total load. Therefore the composite's yield stress depends on the effective load bearing cross section, which is the maximum value of the matrix area in the cross-section perpendicular to the load direction. It is for this reasons that theoretical analysis of simple models gives no satisfactory description of the yield stress as function of the composition [1, 14, 16].

Interfacial adhesion between the matrix and filler is of primary importance for load transfer between these phases. It is, however very difficult to measure. Therefore filler/matrix adhesion is often inferred only qualitatively by examining the interfacial aspects at fracture surfaces, or simply by measuring whether or not the mechanical properties of the composites are greater than those of the matrix [32]. Many scientists were faced with a challenge to obtain a more rigorous approach to describe quantitatively the compositional dependence of tensile yield stress in filled polymers [31, 32].

Turcsanyi *et al.* [31] developed a model that will best fit composites reinforced with natural fillers. They worked with composite materials that consist of a matrix polymer as a continuous phase and generally inorganic filler dispersed in the matrix. In their model they have chosen simple hyperbolic functions to describe the change of the effective cross-section as function of filler content. Their equation contains the adjustable parameter A, which can be determined for systems with known  $\varphi^*$  and  $\psi^*$  values (respectively the filler volume fraction and filler area fraction in the cross-section) in the following expression:

$$(1 - \psi^*) = (1 - \varphi^*) / (1 + A \varphi^*) \quad (1.1)$$

Since the packing of the fillers depends on particle size distribution, and since it can vary from sample to sample, they tested different samples and found the value of A in the range 2.318 to 2.427. They chose a value of A = 2.5 as an upper limit. They found a linear dependence of yield stress on the filler content in most cases that they have worked with. They also came up with an exponential function that best described this dependence

$$\sigma_c = (1 - \varphi) / (1 + 2.5\varphi) \sigma_0 \exp \{B\varphi\} \quad (1.2)$$

where  $\sigma_c$  and  $\sigma_0$  are yield stress of the composites and pure polymer respectively, while B is a constant. Although B has no direct physical meaning, they connected its value to the interfacial properties of the given system and to the yield stress of the matrix. They realized that surface treatment, which increased the adhesion between the phases, resulted in a higher value of B. They

carried on to investigate the use of the model on composites containing anisotropic particles and found that it was giving satisfactory results in studying interactions at polymer/filler interfaces.

D'Almeida and Carvalho [32] extended on the validity of the equation developed by Turcsanyi *et al.* [31], for the yield strength evaluation of particulate composites. They studied the ultimate tensile strength of composites that do not show large macroscopic plastic behaviour, and developed a good correlation between the theoretical values derived from the equation and their experimental results on composites filled with both surface treated and untreated particles. They made composites with volume fractions of filler ranging from 4 to 25 %. These fillers (calcium carbonate, atapulgite, sepiolite and short length sisal fibres) were dispersed in matrices of PP, LDPE, MDPE and HDPE. They obtained a dimensionless parameter related to the filler/matrix interface and used it to judge the effectiveness of surface treatment employed in order to enhance the mechanical properties of several particulate filled composites. They also realized that the B parameter could serve as a measurement of the reinforcement efficiency of the filler. Their work was based on the assumption that the approach proposed by Turcsanyi *et al.* [31] is valid when the composite have a macroscopic brittle behaviour and no gross yield deformation occurs. They found that only PP based composites showed large plastic deformation, and sisal fibres had deleterious effects upon the tensile strength of HDPE composites. Sisal fibre displays a differing aspect ratio from other reinforcements. Based on this fact, the shape parameter for sisal fibres had to be considerably different from those obtained for other particulate reinforcements. For these reasons it is necessary that the shape parameters must be left as an adjustable variable when using the proposed model. However, they found that the tensile strength behaviour of particulate filled composites follows the modified model equation proposed by Turcsanyi *et al.*

Ultimate tensile properties are often used for the characterization of polymers and polymer composites. Pukanszky [33] studied factors that influence the ultimate tensile properties of polymer composites, and developed a quantitative model describing the composition dependence of the tensile strength. His results showed that the decrease in specimen cross-section during elongation, the decrease in the effective load-bearing cross-section as an effect of filling, the increase in strength due to the orientation of the matrix, also referred to as strain hardening, and polymer-matrix interaction all determine the tensile strength of a polymer composite.

Felix and Gatenholm [34] conducted a study on the effect of cotton cellulose fibre on the crystallization behaviour of isotactic polypropylene from the melt. They observed that the cotton fibres acted as nucleating agents, and that a transcrystalline phase was created around the fibres. It

was found that the presence of a transcrystalline interphase tremendously improved the shear transfer between fibre and matrix, depending on the thickness of the transcrystalline layer. Their findings have practical applications for the manufacture of cellulose fibre-thermoplastic composites.

Mishra *et al.* [29] further observed that Young's modulus increases with an increase in fibre content, showing a more pronounced increase in treated fibre composites. There is a sharp increase in Young's modulus of untreated banana fibre, while hemp and sisal fibres show little increase. The values are more or less equal up to 50 % fibre content. Young's modulus of composites of hemp and sisal fibre is more or less equal up to 5 % fibre content; where after sisal fibre shows a maximum value for Young's modulus. Young's modulus of the composites increases in the order sisal > hemp > banana at higher concentrations of the fibre in the composites. The impact strength and shear hardness were found to be higher in the treated than in the untreated fibre composites. It was observed that the tensile strength of hemp and sisal fibre composites is greater than for the banana fibre composites, with varying fibre content. The tensile strength of the treated fibre composites is also higher than that of the untreated fibre composites. It was observed that mechanical properties decrease when the fibre loading gets higher than what the composite can contain. This study showed that a better quality of plant fibre-reinforced composites could be obtained by MA treatment.

MacKenzie and Scanlan [35] investigated the stress relaxation in carbon-black filled rubber vulcanisates, which are known to give an increase in the viscoelastic response to deformation, increased creep, and stress relaxation. They showed the existence of a distinct relaxation process that occurs within the first 60 seconds of relaxation at room temperature. This process becomes less important as the strain is increased and disappears when the temperature is increased or the rubber is swollen. It was suggested that this relaxation was the result of the breakdown of the structure formed in the presence of the carbon-black particles.

Varghese *et al.* [36] studied stress relaxation behaviour of chemically treated short sisal fibre-reinforced natural rubber composites and the effect of bonding agent, strain level, fibre loading, fibre orientation and temperature. Their results showed the existence of a single relaxation pattern in the unfilled stock, and a two-stage relaxation mechanism for the fibre-filled composites. The initial relaxation occurred at short times (< 200 s), and the second-stage relaxation took much longer. The initial mechanism is due to the fibre-rubber attachments, and the latter to physical and chemical relaxation processes of natural rubber molecules. The relaxation process is influenced by the bonding agent, which indicated that the process involved a fibre-rubber interface. For the

composites in the presence of a bonding agent, the rate of relaxation increases with strain level. However, in the presence of a bonding agent, the relaxation rate is almost independent of strain level because of the strong fibre-rubber interface. The initial rate of the stress relaxation process diminished after ageing.

## 1.6 Chemical treatment of fibres

Natural fibre-reinforced thermoplastic composites are more economic to produce than original thermoplastics. It may therefore be possible to meet any future shortage of thermoplastics. The use of natural fibres in thermoplastic composites is highly beneficial, because the strength and toughness of the plastics can be improved. However, a lack of good interfacial adhesion and poor resistance to moisture absorption made the use of natural fibre-reinforced composites less attractive. This problem can be overcome by treating these fibres with suitable chemicals. Cellulosic fibres are reported to be generally incompatible with hydrocarbon polymers, due to the hydrophilic nature of cellulose fibres and the hydrophobic nature of thermoplastics. Several treatments were reported to improve the fibre-matrix interfacial bonding.

Joseph *et al.* [37] investigated the effect of chemical treatment of the fibre on the tensile properties of sisal fibre-reinforced LDPE composites by using chemicals such as sodium hydroxide, isocyanate, permanganate and peroxide. This was an attempt to improve the bonding at the fibre-polymer interface. Their results showed a considerable enhancement of the tensile properties of the composites, but to varying degrees. It has been shown that treatment reduced the hydrophilic nature of the sisal fibre and thereby enhanced the tensile properties of the LDPE-sisal composites. It has also been found that a low concentration of permanganate in the LDPE-sisal system during mixing considerably enhanced the mechanical properties. The tensile strength and modulus of alkali treated and untreated composites showed an increase with fibre loading. Alkali treated fibre composites showed more superior tensile properties than untreated composites. The observation was attributed to the fact that alkali treatment improves the fibre surface adhesive characteristics by removing natural and artificial impurities, thereby producing a rough surface topography. It was also interesting to note that alkali treated LDPE-sisal composites showed superior tensile properties than untreated composites at all fibre lengths. The strength and modulus of the composites showed an enhancement in their values by increasing the average fibre length from 2.1 to 5.8 mm, followed by a decrease in properties when a fibre length of 9.2 mm was used. The results indicated that there exists an optimum fibre length between 5.8 and 9 mm at which a maximum improvement in the properties of the composites can be achieved. They also found that the cardanol derivative of

toluene diisocyanate (CTDIC) treated composites exhibit much better tensile strength and modulus than alkali treated and untreated composites at 30 % fibre loading and 5.8 mm fibre length.

Peroxide treatment was done by adding a 10 % NaOH solution to the chopped fibres, and stirring it for 1 hour. The fibres were then washed with distilled water containing a small amount of acid, after which they were soaked with 1L of a 6 % solution of DCP in acetone. The solution was decanted and the fibres dried, after which the fibres were blended with LDPE. These composites showed an enhancement in tensile properties at 30 % fibre loading. For example, the tensile strength of DCP treated randomly oriented fibre composites is 21.8 MPa, which is 50 % more than the tensile strength of the untreated composites (14.7 MPa). The modulus values of the treated composites also show a similar trend. Permanganate treated composites showed a similar trend, respectively due to peroxide and permanganate induced grafting. It was seen that tensile strength reaches a maximum at a permanganate concentration of 0.055 %, and then decreases sharply with further increase in concentration due to the degradation of cellulosic fibres at higher permanganate concentrations. Among the various types of treatments, CTDIC and DCP treatments showed better tensile properties than other chemically treated sisal fibre composites. The property increases as a result of various treatments vary in the order DCP > CTDIC > BP > KMnO<sub>4</sub> > alkali.

Joseph *et al.* [37] also studied the effect of ageing on the mechanical properties and dimensional stability of the cardanol derivative of toluene diisocyanate (CTDIC) treated and untreated LDPE-sisal composites. They evaluated the tensile properties and dimensional stability under two different ageing conditions. In the first case the samples were immersed in boiling water for 7 hours under atmospheric pressure, while in the second case samples were heated at 70 °C in an air-circulating oven for 7 days. It was discovered that the CTDIC treated composites showed superior mechanical properties and dimensional stability, compared to untreated composites under identical conditions. The greater resistance of the composites with treated fibre under different ageing conditions indicated the existence of an efficient interfacial area between the fibre and the polymer matrix. This implies that suitable fibre surface treatment is necessary for improved mechanical properties and dimensional stability of sisal fibre filled-LDPE composites. They finally observed that these composites have a wood-like appearance and can be used as a substitute for wood.

Li [5] concludes that fibre-surface treatment can improve the adhesion properties between sisal fibre and the matrix, and simultaneously reduce water absorption [9, 10]. He showed the relationship between surface treatment and tensile properties of sisal fibres. His modification methods include alkali, H<sub>2</sub>SO<sub>4</sub>, combined H<sub>2</sub>SO<sub>4</sub> and alkali, benzol/alcohol de-wax treatment,

acetylated treatment, thermal treatment, alkali-thermal and thermal-alkali treatments. Thermal treatment (at 150 °C for 4 h) seems to be the most desirable method in terms of strength and modulus properties, because of the increased crystallinity (from 62.4 % for untreated to 66.2 % for 150 °C / 4 h treated) of sisal fibres. When the temperature reaches 200 °C, the tensile properties will decrease as a result of the degradation of fibres. Other treatments increase the ductility of sisal fibres substantially, but decrease the modulus. It was found that the treatment of sisal fibres in silane, preceded by mercerization, provides improved wettability, mechanical properties and water resistance of sisal-epoxy composites. The treatment in 100 % silane produced fibres that are almost hydrophobic. This meant that the treatment improved interfacial bonding, playing an important role in reducing water absorption in cellulosic fibre-reinforced composites.

Formation of entanglements at brush-like interfaces in cellulose-polymer composites was studied in an attempt to counter the incompatibility of hydrophilic cellulose fibres and hydrophobic thermoplastic matrices, which yielded composites with poor properties [39]. Cellulose fibres were grafted with compatibilizing agents, such as maleated polypropylenes of different molecular weights. The molecular weight of maleated polypropylene (MAPP) compatibilizer, used for cellulose surface treatment, was found to be crucial for adhesion in cellulose-polypropylene composites. In all cases the compatibilizing agent was immobilized on the cellulose fibre surface by chemical bonding. Steric effects and surface free-energy effects were found to stimulate the stretching of grafted chains away from the cellulose fibre surface, giving rise to a brush-like configuration in a polypropylene melt. Dynamic mechanical measurements and tensile testing of composites showed that the presence of a compatibilizing agent considerably enhanced stress transfer and increased interface thickness, the most significant effect being obtained for the high molecular weight compatibilisers. The longer the grafted chains, the larger the fraction of matrix molecules involved in the interaction and the thicker the interphase. The improvement of adhesion between treated fibres and PP, as detected by peel testing, were proven to be caused mainly by entanglements formed between the compatibilizing agent and PP.

Matrix substrates, which play a role in filled polymer systems, have also been a subject of intensive research. These substances, when used in their virgin state, were found to produce a poor interface with cellulose fibres resulting in poor mechanical properties. In an attempt to arrest this problem, Mwaikambo *et al.* [40] used kapok/cotton fabric as reinforcement for conventional polypropylene and maleic anhydride grafted polypropylene resin. They treated the samples with acetic anhydride and sodium hydroxide to modify the fibre (or fabric). It was evident from their results that fibre modification gave a significant improvement in the thermal properties of the plant fibres, whereas

tests on the mechanical properties of the composites showed poor tensile strength. Mercerisation and weathering were found to impart toughness to the materials, with acetylation showing slightly less rigidity compared to other treatments on either the fibre or composites. The modified polypropylene improved the tensile modulus and had the least toughness of the kapok/cotton reinforced composites. The incorporation of maleic anhydride on the polypropylene molecule improves the fibre matrix interfacial adhesion and composites stiffness, and increases in the tensile modulus at higher fibre content. A comparison between the glass reinforced–maleic anhydride isotactic polypropylene (MaiPP) composites and the polypropylene composites shows that glass fibre gives higher flexural properties on the MaiPP matrix than kapok/cotton fabric.

## **1.8 Objective of the study**

Fibre reinforced composites are a very intensively studied area, which proved to have big practical importance worldwide. The reason for this is that most organic fillers are natural components, which are mostly renewable, and very cheap. The fibre-reinforced composites are also reported to be biodegradable, which is mostly desired because it is safe to work with them for they have no health hazard [5, 14]. In recent years there has been an increasing interest in finding new applications for sisal-fibre reinforced composites, which are traditionally used for making mats, ropes, carpets and fancy articles [2]. Sisal fibre was chosen as a natural reinforcer on account of its excellent mechanical properties, for instance low density, high specific strength and modulus. There are no reported health risks associated with sisal fibre, and this fibre is chosen also for its low cost, easy availability and renewability. Besides the fact that sisal fibre is vastly used worldwide, it has been proven that it is still under-utilized. There are presently great interest amongst materials scientists and engineers regarding its use as reinforcement in composites.

The objective of the study is to investigate the effect of sisal fibre and DCP on the mechanical and thermal properties of sisal fibre reinforced LLDPE composites. It is important to note the importance of surface treatment or modification processes for adhesion enhancement of the resulting composites. A great deal of controversy has been generated over the years as to the reason for the poor initial adhesion of the polymers, the effects of the pre-treatments, and the reason for the enhanced adhesion performance. The project will attempt to answer some of these questions.

The addition of cross-links leads to stiffer, stronger, tougher products, usually, in the case of rubbers, with enhanced tear and abrasion resistance. This is normally the case whether carried out by chemical cross-linking in an unmodified amorphous polymer system, or by addition of



reinforcing filler. However, extensive cross-linking in a crystalline polymer may cause loss of crystallinity, with resulting deterioration of the mechanical properties depending on this factor. When this occurs, the initial trend may be towards either enhancement or deterioration of properties, depending on the degree of crystallinity of the unmodified polymer and the method of formation and location (crystalline or amorphous regions) of the cross-links. Another objective of the study is to investigate and explain the influence of sisal fibre as well as the effect of the DCP treatment on the crystallinity of the composites.

Understanding the factors controlling the strength and toughness of polymers has led to improvements in materials properties, and also to polymers being accepted as structural engineering materials in their own right. Natural fibres compete with polymer fibres, produced with extremely high levels of stiffness and strength, and rank among the strongest materials known. This forms the basis for choosing sisal fibre as reinforcement in this study as an attempt to form composites with improved mechanical properties.

In this project short sisal fibre is used as a reinforcement and the effect of increasing sisal content on both the mechanical and thermal properties of the formed composites will be investigated. LLDPE, is used as a matrix and DCP is used in small quantities as a free radical cross-linking and/or grafting initiator.

To provide information about the visco-elastic properties of the composite materials, various experimental techniques were implemented. DSC and DMA were used for thermal analysis of these composites, and tensile testing for analysis of the tensile strengths and stress relaxation of the materials. FTIR analysis helped in revealing the structure of the reinforced composites.

## CHAPTER 2

### MATERIALS AND METHODS

#### 2.1. Materials

Sisal (*Agave sisalana*) fibre was obtained from the National Sisal Marketing Committee in Petermaritzburg, South Africa. These were supplied as very strong cream-white fibres. The physical and mechanical properties of sisal fibre are given in Table 2.1.

**Table 2.1 Properties of sisal fibre and LLDPE**

Substance	d / ( $\mu\text{m}$ )	$\sigma$ / (MPa)	E / (MPa)	$\epsilon_b$ / (%)
Sisal	100-300	490	11350	5
LLDPE	-	11.4	151.0	533.0

d = Fibre diameter

E = Tensile modulus

$\sigma$  = Tensile strength

$\epsilon_b$  = Elongation at break

The fibre was chopped into small pieces that fitted in a CYCLOTEC 1093 sample mill for grinding. Because discontinuous short sisal fibre is needed for reinforcement, fibres were chopped to reduce the fibre length to diameter ratio. Sisal powder was first soaked in petroleum ether at 40 °C for 4 to 5 hours, with regular shaking, and then washed thoroughly with warm distilled water. It is important to remove all unwanted material, including wax. Finally the fibre was oven dried at 80 °C.

LLDPE, with an MFI of 3.5 g/10 min at 190 °C, 2.16 kg and a density of 0.938 g cm<sup>-3</sup>, was supplied by Sasol Polymers in a powder form. It has a particle size less than 600  $\mu\text{m}$ , and an average molecular weight of 191600 g.mol<sup>-1</sup> (see Table 2.1 for mechanical properties).

Dicumyl peroxide (DCP), which was supplied by Sigma Aldrich, has the molecular formula [C<sub>8</sub>H<sub>5</sub>C(CH<sub>3</sub>)<sub>2</sub>]<sub>2</sub>O<sub>2</sub>, with a formula weight of 279.37, an assay of 98 % and a melting point of 39.4 °C. It decomposes at temperatures above 88 °C.

#### 2.2. Composite preparation

The LLDPE-sisal composites, with and without the presence of DCP, were prepared by mechanical mixing in a coffee mill for about 2 minutes. The samples were then melt pressed into 100 x 80 x

0.7 mm shapes at 180 °C for 10 min using an AMS 10-ton hot melt press. Table 2.2 outlines the different samples, as they were prepared in different mass ratios.

**Table 2.2 Mass ratios of samples used in this study**

LLDPE/DCP/sisal	LLDPE/DCP/sisal	LLDPE/DCP/sisal
50/0/50	49/1/50	47/3/50
60/0/40	59/1/40	57/3/40
70/0/30	69/1/30	67/3/30
80/0/20	79/1/20	77/3/20
90/0/10	89/1/10	87/3/10
100/0/0	99/1/0	97/3/0

The composites were then cut into dumbbell shaped samples that were on average 75.8 mm long, with a gauge length of 24 mm and cross-sectional area of 7.54 mm<sup>2</sup>.

### 2.3. Characterisation and analyses

#### 2.3.1. Gel content

The gel content of the composites was determined through xylene extraction of the uncross-linked parts of the samples. Small samples were cut, weighed, and wrapped in fine stainless steel mesh, which was provided by the Screen Products Division of Meshcape Industries (Pty) Ltd. These wrapped samples were tied with a string and then placed in a round-bottomed flask half-filled with xylene, and refluxed for 12 hours. The samples were suspended or hanged just above the level of xylene throughout the experimental period. Xylene was changed after 6-hour intervals. After the extraction, the wrapped samples were washed with chloroform, air-dried at ambient temperature for 24 hours and then at 50 °C in an oven for 4–5 hours. Once again the samples were weighed and the gel content was determined by using Equation 2.1, in order to find the mass of xylene insoluble gel relative to its initial mass. It was important to disregard the mass of sisal, since sisal does not dissolve in xylene. To calculate the gel % of composites, the mass of PE in the sample before extraction was calculated by first multiplying the sample mass with the value of the PE fraction in the sample. The mass of the mesh, wire and sisal was then subtracted from that of the final non-dissolved sample, mesh and wire. The difference is divided by the original mass of PE in the sample before extraction and multiplied by 100. This is summarised in Equation 2.1.

$$\% \text{ Gel} = [m_3 - (m_2 - xm_1) / xm_1] \times 100 \quad (2.1)$$

where  $m_1$  is the mass of LLDPE before extraction,  $m_2$  the mass of LLDPE + mesh + copper wire before extraction, and  $m_3$  is the mass of LLDPE + mesh + copper wire after extraction and drying.  $x$  is the fraction that excludes sisal.

### 2.3.2. Fourier transform infrared (FTIR)

Samples were characterized on a Nicolet Impact 410 FTIR spectrometer connected to an MTEC Model 300 photo-acoustic detector. Helium gas was used for purging. A resolution of  $16 \text{ cm}^{-1}$ , a scan range of  $4000 - 400 \text{ cm}^{-1}$ , and a total of 200 scans were set as parameters for analysis.

### 2.3.3. Water absorption

Samples were weighed and placed in distilled water at room temperature. Water absorption was monitored every day for a period of 10 days, after which there was no more apparent increase in the mass of the samples. The samples were removed from the water, dried by blotting and weighed, and then returned to the distilled water, which was changed every day. Percentage moisture uptake was calculated according to Equation 2.2.

$$\% M_t = [(W_w - W_d) / W_d] \times 100 \quad (2.2)$$

where  $M_t$  is the total moisture uptake,  $W_d$  is the initial weight of the sample, and  $W_w$  are the weights determined after different times  $t$  of immersion.

### 2.3.4. Dynamic mechanical analysis (DMA)

The softening points were tested using a Perkin-Elmer method on a Perkin-Elmer DMA-7e. Samples were subjected to a static force of 5000 mN and a dynamic force of 10 mN, and a frequency of 10 Hz was used. The samples were then heated from 50 to 180 °C at a rate of  $5 \text{ °C min}^{-1}$ .

### 2.3.5. Differential scanning calorimetry (DSC)

Differential scanning calorimetry was carried out on a Perkin-Ermer DSC-7 thermal analyser in a nitrogen atmosphere. The instrument was calibrated using the onset temperatures of melting of indium and zinc standards, and the melting enthalpy of indium. The samples, approximately 10 mg each, were heated from 25 to 180 °C and maintained at this temperature for 5 min to eliminate thermal history effects. They were then cooled to 25 °C at a rate of 10 °C min<sup>-1</sup>. They were maintained at this temperature for a minute and reheated to 180 °C at the same rate. Melting temperatures and melting enthalpies were determined from the second scan.

### 2.3.6. Mechanical testing

Tensile testing of dumbbell shaped specimens (Figure 2.1) of size 24.0 x 1.64 x 4.6 mm, which denotes the gauge length, thickness and width respectively, was carried out using a Hounsfield H5KS tensile tester at a cross-head speed of 50 mm.min<sup>-1</sup>. The tensile modulus and elongation at break of the composites were calculated from the force-displacement curves. At least three specimens were tested for each set of samples and the mean values are reported. Force (N) values were converted to stress (MPa) values by dividing them by the sample cross-sectional area  $A$  (mm<sup>2</sup>), whilst elongation  $\epsilon$  was given by the extension in gauge length  $x$  divided by the original gauge length  $x_0$ .

$$\text{Tensile stress (MPa)} = F \text{ (N)} / A \text{ (mm}^2\text{)} \quad (2.3)$$

$$\% \text{ Strain or elongation} = [(x_1 - x_0) / x_0] \times 100 \% \quad (2.4)$$

Young's modulus = stress / strain in the linear portion of the stress-strain curve

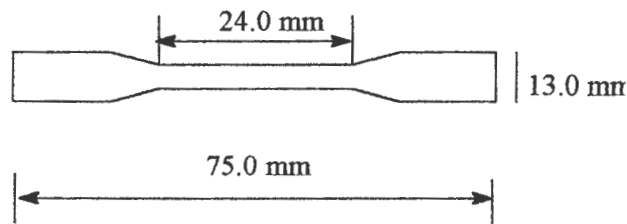


Figure 2.1 Dumbbell-shaped specimen which was used for mechanical measurements

The stress relaxation of samples was analysed by stretching the samples to 1.00 % strain and monitoring the decrease in force as a function of time. The simplest assumption is that the drop in stress follows an exponential decay:

$$\sigma(t) / \sigma_0 = e^{-t/\tau} \tag{2.5}$$

where  $\sigma(t)$  is the stress at time  $t$ ,  $\sigma_0$  the stress at  $t = 0$ , and  $\tau$  a constant called the relaxation time. This equation assumes that the stress will eventually drop to zero. This is, however, not always true, which brings us to a more accurate or better assumption (Equation 2.6).

$$(\sigma(t) - \sigma_\infty) / (\sigma_0 - \sigma_\infty) = e^{-t/\tau} \tag{2.6}$$

where  $\sigma_\infty$  is the stress at infinite time. This equation assumes that the stress eventually drops to a constant value  $\sigma_\infty$ , which must be subtracted from all the stress values before fitting to the exponential decay.

#### 2.3.7. *Microscopy*

Microscopic photos of composites were obtained by means of a Nikon eclipse microscope using 4 x 10 and 10 x 25 magnification.

## CHAPTER 3

### RESULTS AND DISCUSSION

It is well known that the physical properties of polymer composites are largely dependent on adhesion between fillers and the polymer matrix. Non-polar polymers (PE, PP, etc), that are not capable of forming H-bonds with the hydroxyls available on the filler surface, have poor adhesion and wettability to the filler. The efficiency of a fibre-reinforced composite depends on the fibre matrix interface and ability to transfer stress from the matrix to the fibre. This stress transfer efficiency plays a dominant role in determining the mechanical properties of the composites and also in the material's ability to withstand environmentally severe conditions. Additionally, it is important to maintain good stiffness to impact strength balance in order to expand the applicability of these natural fibre-reinforced composites [40]. In this study dicumyl peroxide (DCP) was used as treatment for the sisal fibre in order to improve the adhesion between matrix and filler. The results discussed in this chapter will indicate whether this approach was successful.

#### 3.1 Characterization of composites

##### 3.1.1 Gel content

**Table 3.1** Gel content of uncross-linked and cross-linked LLDPE-sisal composites

LL/D/S	% Gel/w <sub>LL</sub>	LL/D/S	% Gel/w <sub>LL</sub>	LL/D/S	% Gel/w <sub>LL</sub>
50/0/50	1.4	49/1/50	78.2	47/3/50	96.0
60/0/40	0.3	59/1/40	84.9	57/3/40	97.0
70/0/30	1.4	69/1/30	85.9	67/3/30	97.0
80/0/20	0.5	79/1/20	85.5	77/3/20	97.0
90/0/10	1.7	89/1/10	88.1	87/3/10	96.8
100/0/0	0.1	99/1/0	92.7	97/3/0	96.6

LL/D/S = LLDPE/DCP/sisal

% Gel/w<sub>LL</sub> = gel content with respect to LLDPE

Table 3.1 gives a summary of the gel content of both the untreated and treated LLDPE-sisal composites. All the values for the gel content were determined with respect to the LLDPE content by subtracting the sisal content from the total gel. Sisal fibre is insoluble in xylene and it remains in the mesh with the gel. The dependence of the gel content on DCP content in the composites for various sisal concentrations is shown in Figure 3.1. The gel content of samples prepared in the

presence of 3 % DCP seems to be constant, independent of sisal fibre content. However, there is a decrease in gel content with increasing amount of sisal when 1 % DCP was used. This can also be seen in Figure 3.2, which shows the dependence of the gel content on sisal fibre content for 1 % and 3 % DCP respectively. 1 % DCP already gives rise to high gel content, indicating that 3 % DCP may be too much, resulting in polymer degradation. A decrease in gel content, which is observed for 1 % DCP as the sisal content increases, may indicate that sisal fibre separates the LLDPE chains to such an extent that cross-linking is effectively reduced. The fact that such a decrease in gel content is not observed in the case of 3 % DCP treated samples, may indicate that links are formed between LLDPE chains and sisal fibre, as previously suggested by Joseph *et al.* [36].

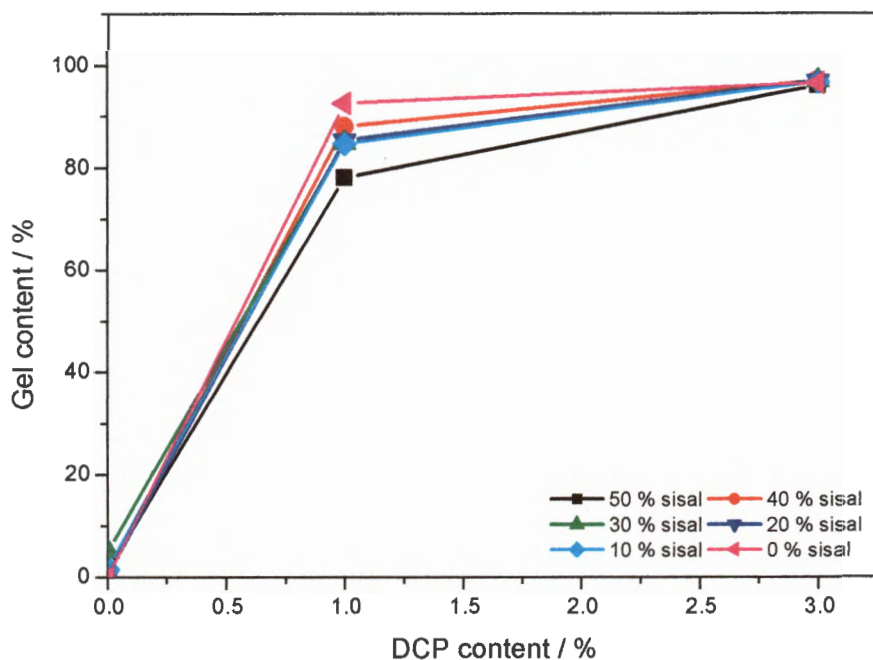


**Figure 3.1** Gel content of cross-linked LLDPE-sisal composites as a function of DCP content



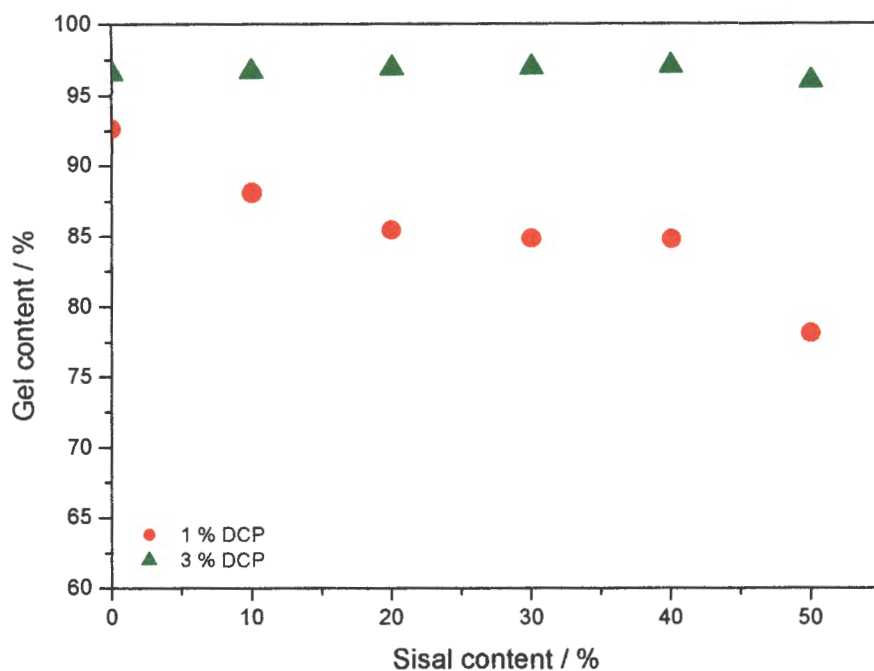


**Figure 3.2 Gel content of cross-linked LLDPE-sisal composites as a function of sisal content**

### 3.1.2 Fourier transform infrared (FTIR)

Figures 3.3-3.5 show typical FTIR spectra of the different samples. The spectrum of pure sisal satisfactorily compares with the FTIR spectrum of pure cellulose reported in literature [6, 9]. The OH band at  $3340\text{ cm}^{-1}$  is observed to be intense and broad for the 100 % sisal sample. The OH band intensity increases with sisal content for all untreated and treated composites. Its peak intensity changes relative to the amount of sisal in the composite. All bands that are characteristic of sisal, that is C=O, C-O and O-H, increase in intensity with increasing sisal content. However, there is no evidence that new bonds had been formed. It is therefore not possible to detect from FTIR measurements any kind of reaction that had occurred.

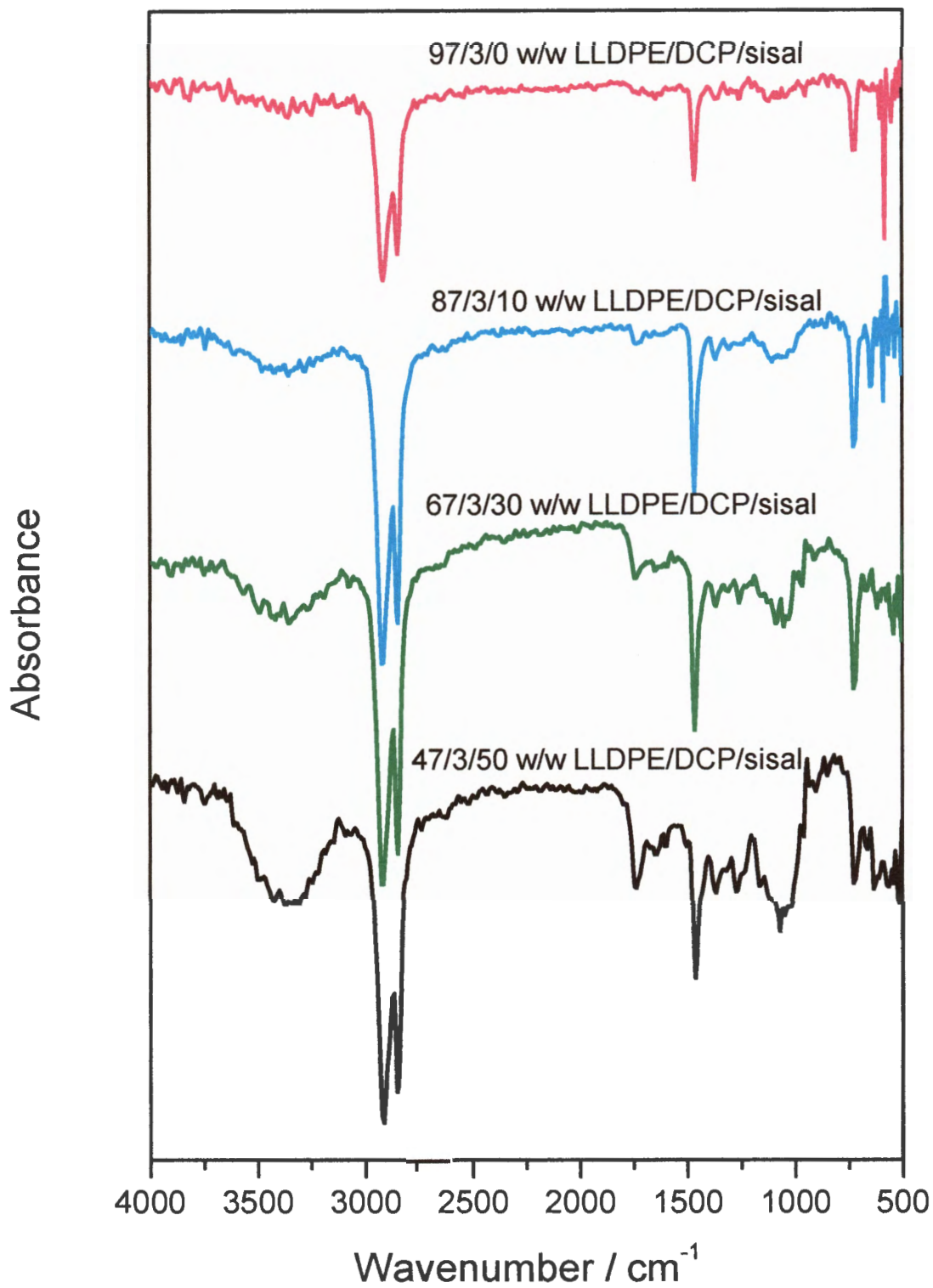


**Figure 3.4** FTIR spectra of LLDPE-sisal fibre composites prepared in the presence of 3 % DCP

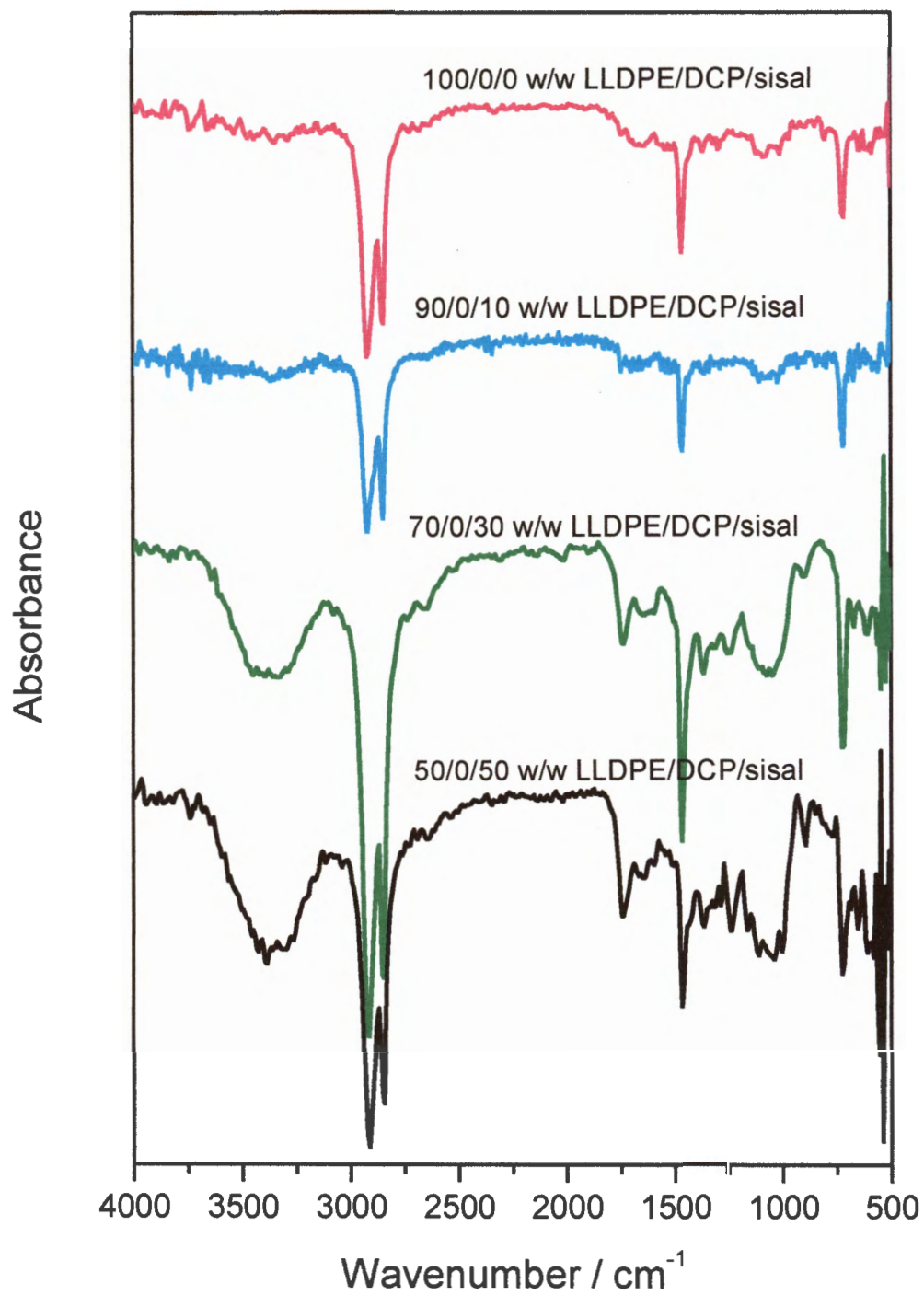


**Figure 3.5** FTIR spectra of untreated LLDPE-sisal fibre composites

Figure 3.3 shows the spectra of the composites reinforced with the same amount of sisal in the presence of varying DCP content. The OH, C=O, C-O bands, that are respectively observed at 3100-3600, 1751, and 1043  $\text{cm}^{-1}$ , seem to decrease in peroxide treated samples. A more pronounced decrease is observed when 1 % DCP is used. The decrease is not so prominent in the case of 3 % DCP treated samples, probably because of oxidative degradation under these conditions, which will contribute to the formation of oxygen-containing groups. There is, however, no significant change in these bands for treated composites with higher sisal content (Figure 3.5). The intensity of the OH group stretching absorption band for all composites with 50 % sisal remained virtually the same. In this case cellulose oh-groups absorb so strongly that the effect of peroxide treatment is not observable in this absorption region. The presence of water in the composites also complicates the interpretation of trends in this absorption region. Li *et al.* [5] mentioned in their study that the strong hydrogen bonding observed at 3390  $\text{cm}^{-1}$  shows an increased degree of fibre-matrix adhesion. This in turn proves that the mechanical properties of the composites are also improved. Their FTIR measurements support the tensile testing results in the sense that the tensile strength increases with fibre content, because interfacial adhesion improves due to more hydrogen bonds formed across the fibre surface. In my case I did not see a separate absorption at 3390  $\text{cm}^{-1}$ , or the intense OH bending vibration in this region overshadowed this absorption.

There is a very pronounced peak at 1746  $\text{cm}^{-1}$  which is associated with the C=O stretching vibration of residual non-cellulosic impurities present in the fibre. The peak seems to be reduced for composites treated with DCP. However, it increases in intensity for 3 % DCP and high (above 30 %) sisal content. This observation concurs with Mwaikambo *et al.* [38] who treated the composites with acetic acid. The increase in intensity at 1735 – 1746  $\text{cm}^{-1}$  is assumed to be due to the presence of the cellulose molecular structure.

At 1043  $\text{cm}^{-1}$  a C-O stretching vibration of the cellulose backbone is observed. The intensity increases with an increase in sisal fibre content for all composites. At higher sisal contents, the peak intensity increases with an increase in DCP content. This may be due to oxidative degradation of the polyethylene matrix in the presence of DCP.

A  $\text{CH}_3$  stretch is observed at 1375  $\text{cm}^{-1}$ . The intensity of this peak is low for pure LLDPE but higher in pure sisal, and it increases with increasing sisal content. This is probably due to the fact that there are more branches in sisal fibre than in the LLDPE matrix. There is no visible change as a result of the addition of DCP to composites having the same sisal content.

There is an increase in the C-H band at  $731\text{ cm}^{-1}$ , with an increase in DCP content. This may be due to a gradual substitution of the hydrogen on the polymer backbone by cross-linking. Peroxide as cross-linking initiator removes the hydrogen from  $\text{CH}_2$  to form CH free radicals. The intensity of the  $1452\text{ cm}^{-1}$  band, assigned to the symmetrical  $\text{CH}_2$  bending, decreases accordingly with an increase in sisal content.

### 3.2 Water absorption of composites

**Table 3.2 Water absorption of the sisal reinforced LLDPE composites**

LL/D/S	% $W_{\text{abs}}$ (24 h)	% $W_{\text{abs}}$ (72 h)	% $W_{\text{abs}}$ (168 h)	% $W_{\text{abs}}$ (216 h)	% $W_{\text{abs}}$ (264 h)
0/0/100	63.6	75.0	77.5	71.3	71.3
50/0/50	21.7	28.5	33.3	32.5	32.4
60/0/40	12.0	17.3	17.8	17.6	17.9
70/0/30	8.2	12.5	15.3	15.7	15.7
80/0/20	4.8	6.5	7.6	7.4	8.7
90/0/10	2.4	3.9	4.8	4.4	4.5
100/0/0	0.4	0.8	0.9	1.0	0.8
49/1/50	12.2	13.2	13.1	13.7	13.7
59/1/40	8.1	7.8	7.9	7.8	8.0
69/1/30	3.6	3.8	4.2	4.2	4.2
79/1/20	2.0	2.2	2.7	2.6	2.6
89/1/10	1.6	2.7	1.4	1.2	1.3
99/1/0	1.6	1.1	1.1	0.6	0.6
47/3/50	10.5	13.2	14.2	13.5	14.2
57/3/40	8.2	9.1	11.0	9.8	11.0
67/3/30	5.0	6.7	8.7	8.1	8.1
77/3/20	2.8	4.5	4.9	5.5	4.5
87/3/10	4.3	3.9	4.8	4.7	4.2
97/3/0	0.6	0.6	0.6	0.9	0.7

LL/D/S = w/w LLDPE/DCP/sisal

Values for percentage water absorption of both treated and untreated LLDPE-sisal fibre composites at different immersion times are given in Table 3.2. It can be seen that water absorption is the highest in pure sisal. Cellulosic fibres are highly hydrophilic in nature. There is a considerable

decrease in water absorption as the composites are formed. However, water absorption is reduced even more when composites are prepared in the presence of DCP. Water absorption is observed to be slightly higher for 3 % DCP treated composites compared to 1 % DCP treated samples. With composites below 30 % sisal content, water absorption is reduced by 68 % on average for composites treated with 1 % DCP, and by 44 % for those treated with 3 % DCP. The higher water absorption in the 3 % DCP treated samples may be the result of polymer degradation, which may lead to the exposure of sisal fibre and the consequent increase in water absorption.

The data is plotted in Figures 3.6 – 3.8 as weight % water absorption of the composites as function of time in days. The water absorption of composites increases with immersion time and increasing sisal fibre concentration. A rapid water uptake was observed for all samples within the first few days of immersion, but this rate decreased slowly with time. Although there appear to be fluctuations between the 8<sup>th</sup> and 11<sup>th</sup> day for some composites, the uptake of water for most composites levels off to a constant value.

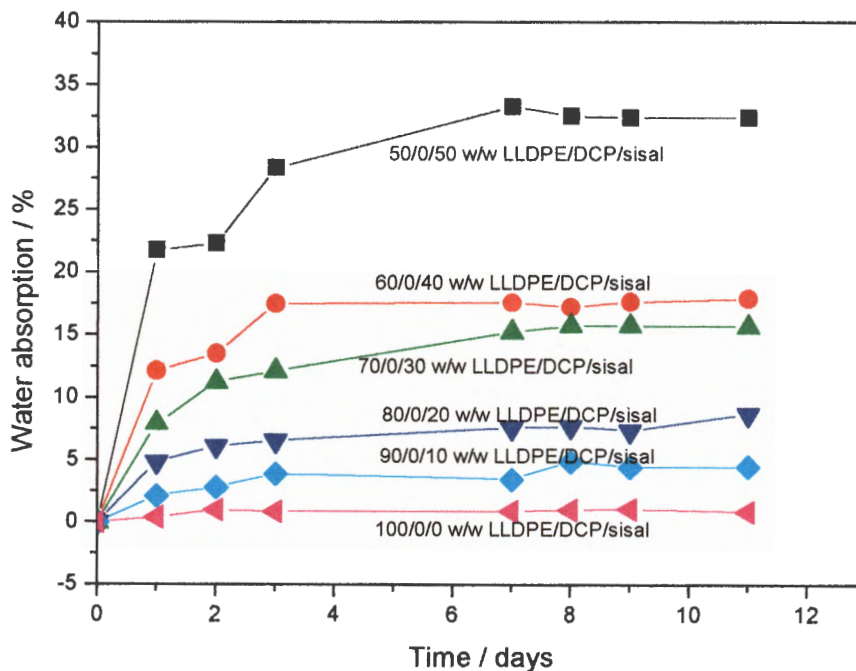


**Figure 3.6. Water absorption of untreated LLDPE-sisal composites as a function of time in days**

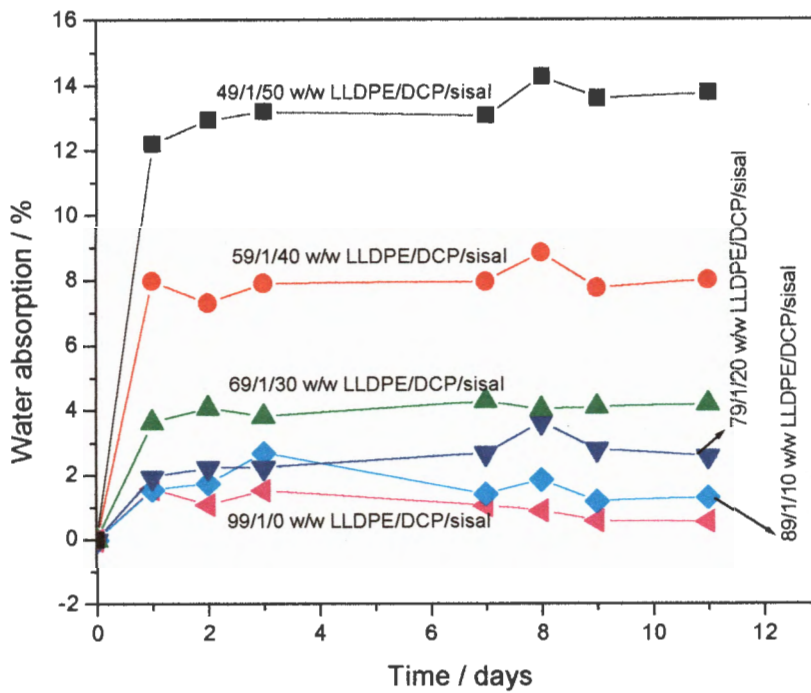


**Figure 3.7** Water absorption of LLDPE-sisal composites treated with 1% DCP as a function of time in days

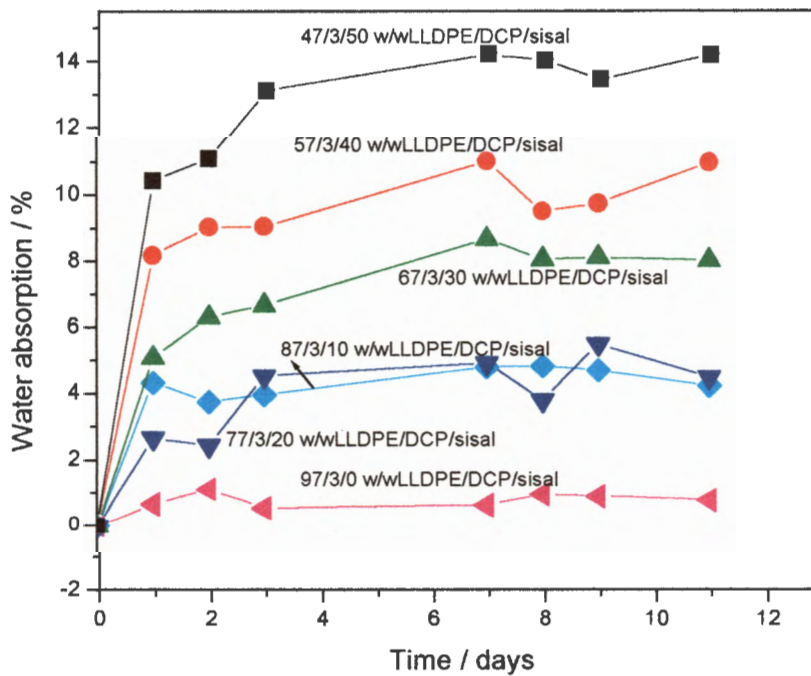


**Figure 3.8** Water absorption of LLDPE-sisal composites treated with 3% DCP as a function of time in days

The influence of DCP content on maximum water uptake for increasing sisal content is shown in Figure 3.9. Water absorption increases with increasing fibre content, but decreases with peroxide treatment. At high fibre contents the water absorption by peroxide-treated composites is much lower than that by untreated composites. The absorption of water is related to its rate of diffusion into the composite. In some way the peroxide treatment inhibits water absorption by sisal fibre in the LLDPE matrix. LLDPE network formation and/or grafting between LLDPE and sisal (as previously suggested by Joseph *et al.* [36]) in some way restricts the diffusion of water to the hydrophilic sisal. For pure LLDPE water absorption is practically zero because of its hydrophobic character.

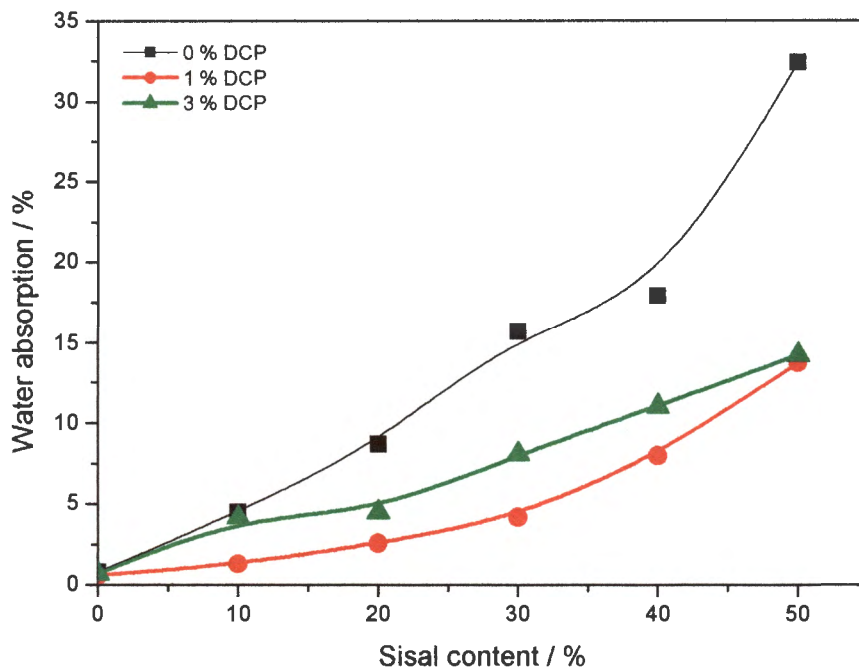


**Figure 3.9** Water absorption after 264 h of the composites as a function of sisal content

At sisal contents of 30 % and above water uptake of composites increases exponentially. This suggests the LLDPE-sisal fibre interfacial adhesion becomes poorer and only improves when treated with DCP. Danjaji *et al.* [30] observed an increase in water absorption with increasing amount of starch granules in LLDPE-starch composites, but in their case it took about 40 days before equilibrium was reached. They realized that water absorption of composites was inversely proportional to LLDPE-fibre interfacial adhesion. They found that at high fibre content, water absorption was high and this also brought about reduction in tensile strength and elongation at break. They argued that the presence of moisture at the LLDPE-starch fibre was weakening the already weak interfacial adhesion. Based on this, the assumption may be made that, because of the



lower water absorption of the DCP treated samples (Figure 3.9), there may be better interfacial adhesion in these samples. Mishra *et al.* [29] investigated the water absorption of untreated and maleic anhydride treated LLDPE composites with hemp, banana and sisal. They found that the order of water absorption was hemp > banana > sisal. They also observed a decrease in water absorption in the case of maleic anhydride treated samples.

It is indeed expected that there will be inhibitory effects on the moisture absorption properties of LLDPE-sisal fibre composites compared to pure sisal fibre, since LLDPE is itself a polymer with a hydrophobic nature and it is reinforced with hydrophilic sisal fibre. The moisture absorption values shown in Tables 3.2 are in accordance with this expectation. If it is assumed, on the other hand, that composites may form grafting between LLDPE and sisal fibre, this will increase with extent of peroxide treatment. The composites with a lower degree of grafting will not show much variation in the moisture absorption values compared to that of the un-grafted composites. With the rise in grafting level, the fibre surface will become increasingly covered with hydrophobic polymer and the moisture absorption capacity will remarkably decrease [11].

### 3.3 Thermal analysis

#### 3.3.1 Dynamic mechanical analysis (DMA)

The dynamic modulus of composites is governed by various factors, for example the matrix type, fibre loading, fibre length, fibre dispersion and fibre-matrix adhesion [5,41]. The DMA determined softening points of the composites are summarized in Table 3.4. It can be seen that the softening point increases with increasing sisal content. However, with a DCP level of 3 %, it looks as if more than 20 % sisal leads to composites that do not show softening behaviour. This may be due to composites becoming more brittle as a large amount of DCP is used.

**Table 3.4 DMA determined softening point values for treated composites**

LL/D/S	Softening point / °C	Probe position / mm
59/1/40	231.96	0.60
69/1/30	147.01	0.47
79/1/20	139.22	0.72
47/3/50	-	-
67/3/30	-	-
77/3/20	145.93	0.37
87/3/10	135.76	0.27

LL/D/S = w/w LLDPE/DCP/sisal - no softening point observed

### 3.3.2 Differential scanning calorimetry (DSC)

**Table 3.5 Thermal properties of untreated and treated LLDPE-sisal fibre composites**

LL/D/S	$T_{o,m} \pm s T_{o,m}$ /°C	$T_{p,m} \pm s T_{p,m}$ °C	$\Delta H_m \pm s \Delta H_m$ / J g <sup>-1</sup>	$T_{o,c} \pm s T_{o,c}$ /°C	$T_{p,c} \pm s T_{p,c}$ °C	$\Delta H_c \pm s \Delta H_c$ / J g <sup>-1</sup>
47/3/50	101.2 ± 1.6	107.7 ± 0.7	29.7 ± 10.4	93.8 ± 1.0	88.5 ± 1.2	-25.7 ± 9.8
57/3/40	103.5 ± 1.0	110.2 ± 0.0	43.7 ± 11.0	96.8 ± 0.4	89.3 ± 0.6	-37.1 ± 9.8
67/3/30	103.6 ± 0.3	111.6 ± 1.2	49.5 ± 14.4	98.1 ± 0.2	91.5 ± 1.3	-35.4 ± 9.8
77/3/20	106.2 ± 3.0	114.2 ± 2.1	46.9 ± 24.5	97.9 ± 1.5	92.3 ± 1.0	-54.75 ± 7.6
87/3/10	106.7 ± 2.3	113.6 ± 1.3	67.2 ± 13.6	99.7 ± 1.4	93.6 ± 1.8	-66.1 ± 18.9
97/3/00	107.2 ± 1.0	115.2 ± 1.0	84.4 ± 19.5	101.1 ± 0.2	90.4 ± 4.9	-70.3 ± 24.9
49/1/50	111.0 ± 2.5	118.4 ± 0.5	49.7 ± 8.6	104.3 ± 0.7	99.3 ± 0.7	-31.9 ± 4.0
59/1/40	110.7 ± 0.5	120.2 ± 0.6	60.7 ± 10.4	105.5 ± 0.7	101.6 ± 1.0	-42.3 ± 3.5
69/1/30	112.0 ± 1.0	121.1 ± 0.2	74.9 ± 11.0	105.8 ± 0.6	101.5 ± 2.0	-51.8 ± 0.9
79/1/20	111.5 ± 0.6	122.3 ± 1.1	84.9 ± 12.3	106.5 ± 0.4	102.7 ± 1.4	-62.8 ± 5.0
89/1/10	112.1 ± 1.7	122.2 ± 0.4	96.3 ± 13.5	107.0 ± 0.8	103.2 ± 2.3	-69.4 ± 2.9
99/1/00	112.1 ± 1.2	122.2 ± 0.2	104.2 ± 17.1	106.8 ± 0.3	103.8 ± 1.0	-81.1 ± 9.8
50/0/50	119.6 ± 1.3	125.6 ± 0.4	60.9 ± 13.7	109.5 ± 1.0	110.1 ± 2.4	-46.7 ± 7.4
60/0/40	120.0 ± 1.2	126.4 ± 0.6	92.4 ± 23.6	109.1 ± 1.2	109.9 ± 2.1	-67.9 ± 13.6
70/0/30	118.8 ± 1.1	125.1 ± 1.2	83.7 ± 16.2	109.3 ± 1.1	109.9 ± 2.3	-71.4 ± 6.6
80/0/20	120.8 ± 1.5	125.4 ± 1.3	110.8 ± 24.4	109.2 ± 1.2	109.9 ± 2.0	-86.0 ± 12.5
90/0/10	120.0 ± 0.8	125.3 ± 0.4	122.6 ± 25.9	108.7 ± 1.3	109.5 ± 1.7	-99.4 ± 10.7
100/0/0	119.7 ± 1.3	124.7 ± 1.3	126.2 ± 24.2	108.3 ± 1.4	109.0 ± 1.7	-108.0 ± 15.1

LL/D/S = mass percentage ratios of LLDPE/DCP/sisal;  $T_{o,m}$  = onset temperature of melting;  $T_{p,m}$  = peak temperature of melting;  $\Delta H_m$  = melting enthalpy;  $T_{o,c}$  = onset temperature of crystallization;  $T_{p,c}$  = peak temperature of crystallization;  $\Delta H_c$  = crystallization enthalpy; s = standard deviations

The DSC heating curves of uncross-linked PE and PE-sisal fibre composites are shown in Figure 3.10. There is only one endothermic peak, which is observed around the melting temperature of LLDPE. This implies that only LLDPE contributes to crystallinity. As expected, the size of the melting peak decreases with increasing sisal content, since only LLDPE melts in this temperature range. Composites, melt pressed in the presence of DCP, show similar behaviour (Figures 3.11 and 3.12). While the melting temperatures of untreated composites slightly increase with increasing amount of sisal fibre, samples treated with 3 % DCP show a decrease in melting temperature. The presence of sisal fibre in the untreated composites obviously favours lamellar thickening, while the formation of a three-dimensional network prevents lamellar thickening during crystallization. If we

the reduced mobility of the PE chains will cause LLDPE to crystallise into thinner lamellar, and this could be the reason for the decrease in melting temperatures ( $T_m$ ) of the samples prepared in the presence of with 3 % DCP.

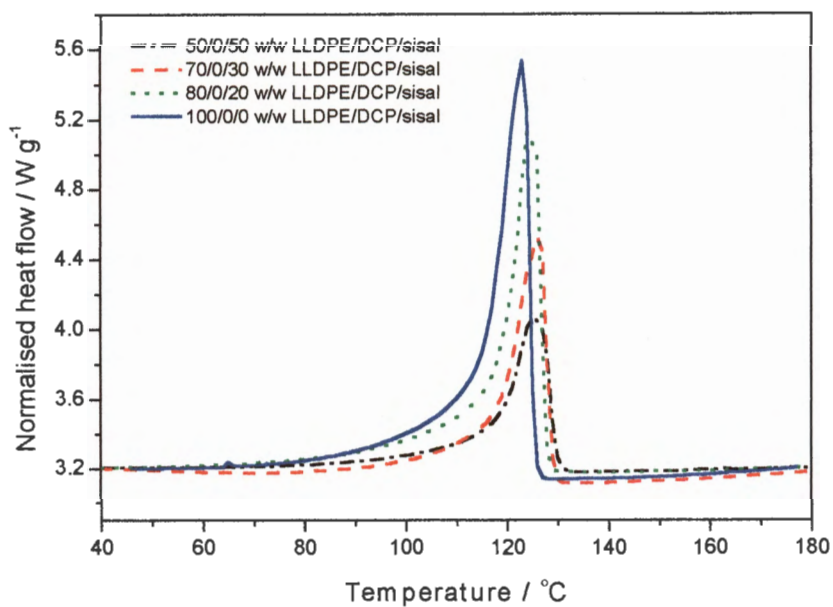


**Figure 3.10** DSC curves of LLDPE and LLDPE-sisal fibre composites (0 % DCP)

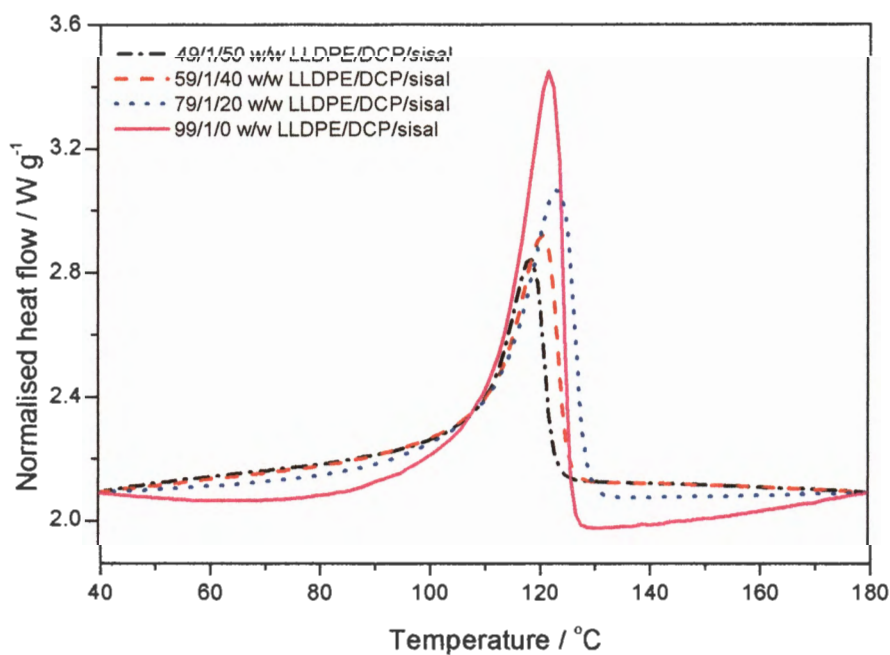


**Figure 3.11** DSC curves of LLDPE and LLDPE-sisal fibre composites (1 % DCP)

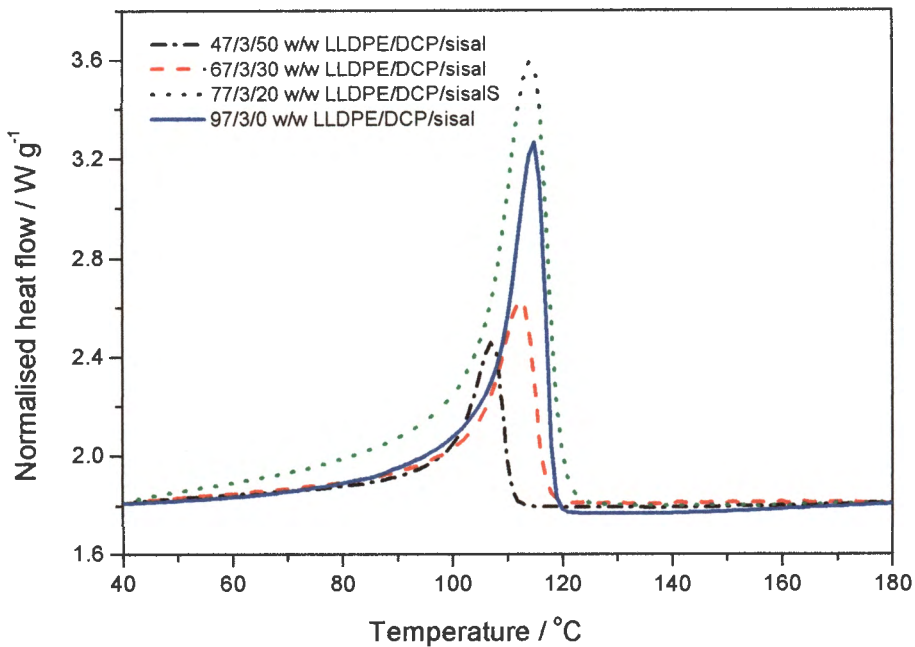


**Figure 3.12 DSC curves of LLDPE and LLDPE-sisal fibre composites (3 % DCP)**

In order to check the influence of the sisal content and peroxide on the melting behaviour of the composites, melting temperatures and melting enthalpies are plotted vs. sisal content (Figures 3.13 to 3.15). Figures 3.13 and 3.14 show, respectively, the onset and peak temperatures of melting of the untreated composites. The melting temperature seems to be fairly constant with increasing sisal content for untreated composites. For the DCP treated samples the melting points are fairly constant for samples containing up to 20 % sisal, after which there is a decrease with increasing sisal content. This is probably due to a disruption in the LLDPE crystal structure in the presence of high amounts of sisal. As expected, DCP treatment gives rise to lower melting temperatures, because it gives rise to lower crystallinity and thinner lamellae. The low melting temperatures for composites with high sisal and DCP contents may also be the result of LLDPE-sisal grafting, as previously suggested by Joseph *et al.* [36]. Such grafting will contribute to a decrease in crystallinity and lamellar thinning. The decrease in melting enthalpy (Figure 3.15) is the direct result of decreasing LLDPE in the composites. The lower enthalpies for DCP treated samples are the result of LLDPE cross-linking which leads to lower crystallinity.

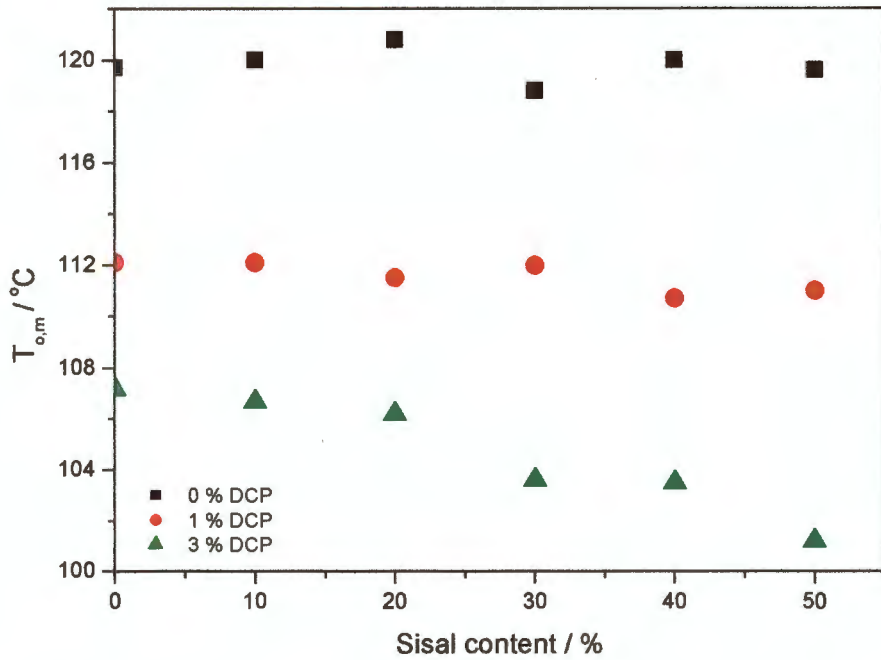


Figure 3.13 Onset temperatures of melting as function of sisal content

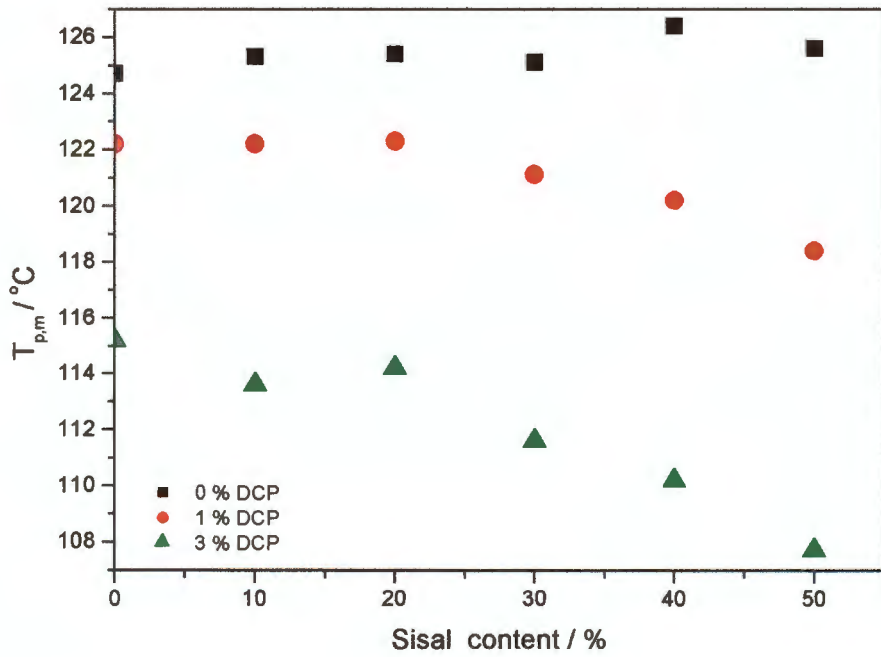


Figure 3.14 Peak temperatures of melting as function of sisal content

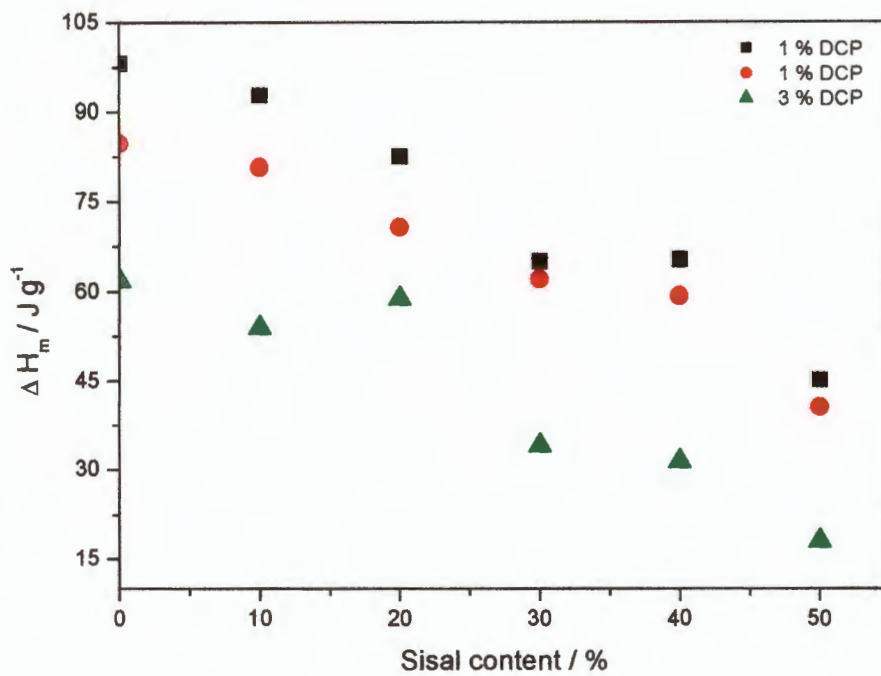


Figure 3.15 Melting enthalpies as function of sisal content

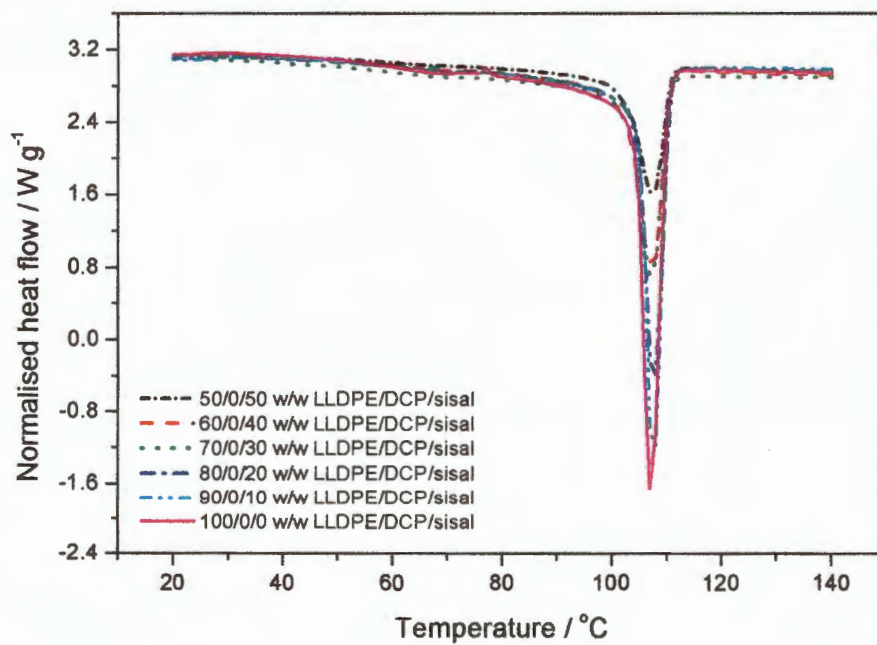
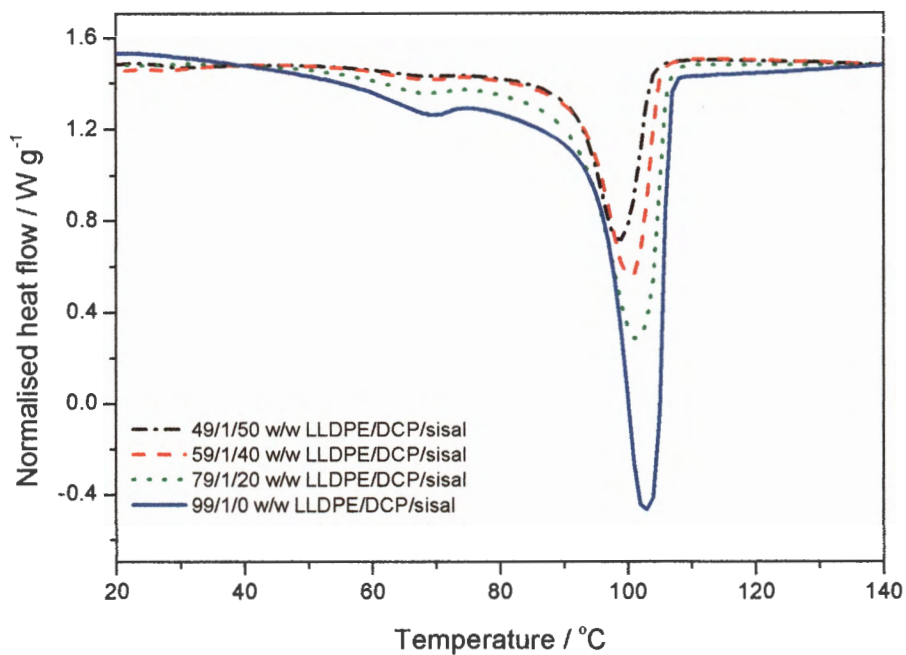
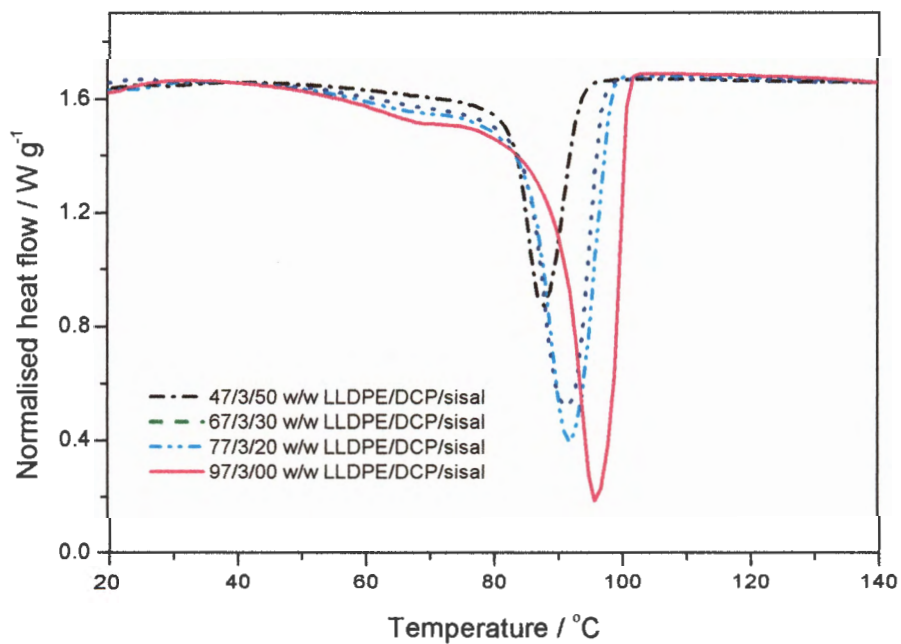


Figure 3.16 DSC cooling curves of LLDPE-sisal fibre composites (0 % DCP)



**Figure 3.17 DSC cooling curves of LLDPE- sisal fibre composites (1 % DCP)**



**Figure 3.18 DSC cooling curves of LLDPE- sisal fibre composites (3 % DCP)**

Figures 3.16 to 3.18 show the DCS cooling curves of the composites, while Figures 3.19 to 3.21 summarise the influence of sisal and DCP content on the crystallization temperatures and enthalpies of the composites. The trends are the same than for the heating curves, and the explanations will be the same.

In Figures 3.17 and 3.18, which are the DSC curves for the treated samples, we observe a small peak around 70 °C. These peaks appear only for pure LLDPE, and LLDPE treated with DCP, and they diminish with increasing sisal fibre content. Krupa and Luyt [53] also observed the development of this peak. However, the reason behind has not been found yet. The only possible explanation was that the development of the peak could be due to the history of the sample.

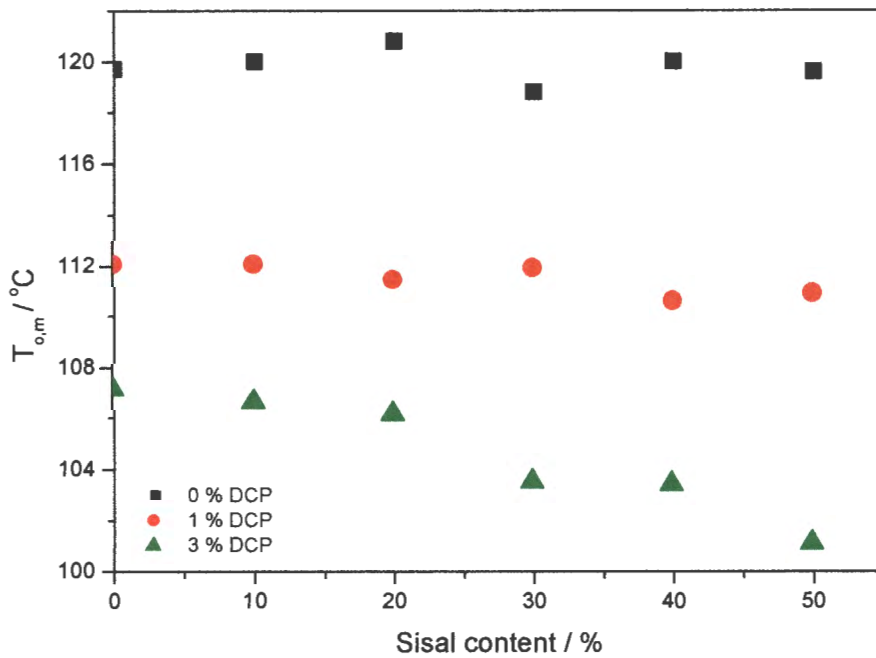


**Figure 3.19** Onset temperatures of crystallization as function of sisal content



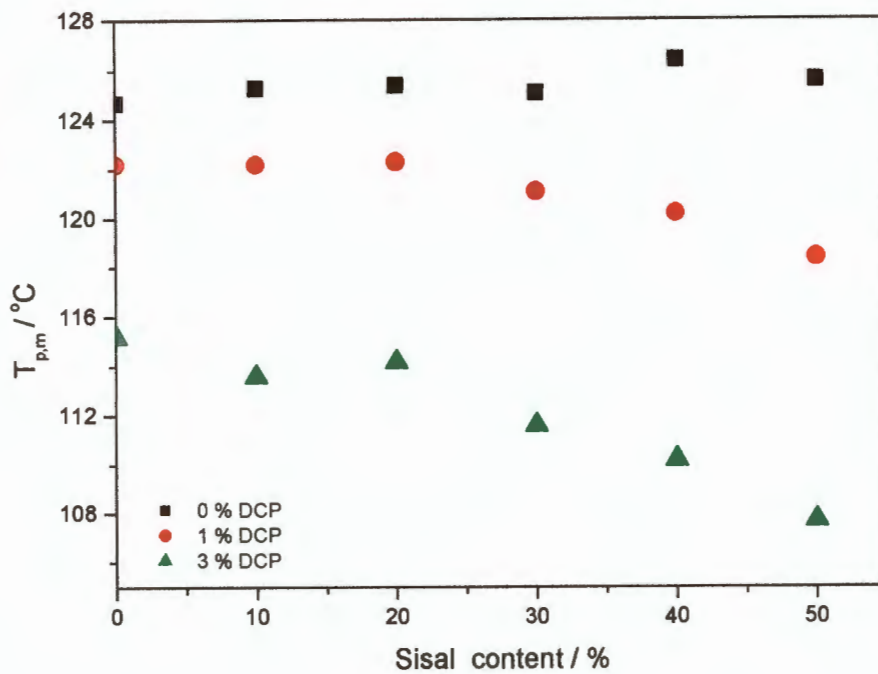


Figure 3.20 Peak temperatures of crystallization as a function of sisal content

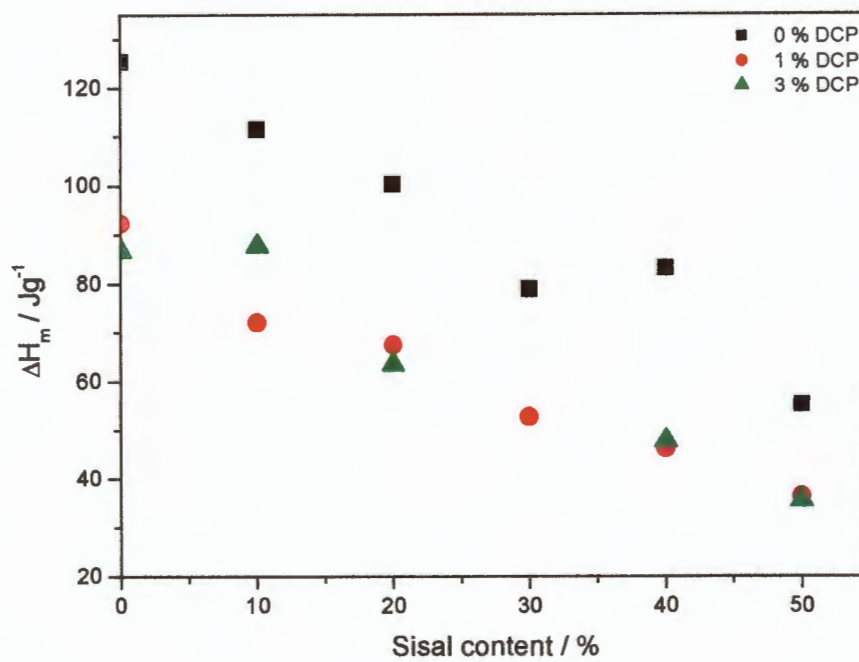


Figure 3.21 Crystallization enthalpies as function of sisal content

Three different DSC analyses were performed on each composite, using samples from different positions on the melt-pressed plate. The onset and peak temperatures of melting have small standard deviation values (Table 3.5), but the melting and crystallization enthalpies have large standard deviation values. This indicates that the sample homogeneity was not very good. This may be improved by melt-mixing the samples in, for example, a Brabender melt-mixer or extruder. In the presence of increasing amounts of sisal, the standard deviation values decrease, which is to be expected, because more sisal will distribute more evenly in the polymer matrix.

### **3.3 Mechanical testing**

#### *3.3.3 Tensile strength*

The elongation at break values are summarised in Table 3.6. Elongation at break of the composites is low, and it decreases with an increase in sisal content. However, it remains fairly constant for all untreated composites. Figures 3.22 and 3.23 respectively show the elongation at break of the composites as a function of sisal and DCP content. DCP treatment of the composites, which leads to cross-linking and possibly also grafting, gives rise to an increase in the elongation at break. At low sisal contents, when the effects of cross-linking are more pronounced, elongation at break is significantly higher than in the untreated composites. An increase in sisal content for DCP treated samples reduces elongation at break, but still to values that are higher than that of the untreated samples. A possible reason for the reduced elongation at break as sisal content increases is the weak LLDPE-sisal interface, which is slightly improved after DCP treatment. Similar results were obtained for the composites with alkali treated sisal fibres [36], where elongation at break was significantly higher than in the untreated composites at low sisal content. Mwaikambo *et al.* [38] observed similar behaviour, where the material (MaiPP) reinforced with untreated fibre, showed less elongation at break compared with composites reinforced with treated fibres. Treatment forms a ductile interface combined with good fibre-matrix interfacial adhesion. In untreated composites the interfacial bond strength is reduced, leading to lower stress resistance.

**Table 3.6 Elongation at break of the LLDPE -sisal fibre composites**

LL/D/S	$\epsilon_b \pm s\epsilon_b / \%$	LL/D/S	$\epsilon_b \pm s\epsilon_b / \%$	LL/D/S	$\epsilon_b \pm s\epsilon_b / \%$
100/0/0	533.0 ± 54				
90/0/10	5.6 ± 1.3	89/1/10	11.8 ± 1.0	87/3/10	19.2 ± 0.4
80/0/20	5.8 ± 1.3	79/1/20	9.2 ± 0.4	77/3/20	9.3 ± 2.1
70/0/30	5.2 ± 2.1	69/1/30	7.6 ± 1.2	67/3/30	8.5 ± 1.7
60/0/40	5.0 ± 0.8	59/1/40	7.0 ± 0.9	57/3/40	6.8 ± 2.1
50/0/50	4.4 ± 0.4	49/1/50	7.2 ± 1.4	47/3/50	6.3 ± 1.6

LL/D/S = mass percentage ratios of LLDPE/DCP/sisal

s = standard deviations

The data for stress at break are summarised in Table 3.7. Figures 3.24 and 3.25 show plots of stress at break of composites as function of respectively sisal and DCP content. It can be seen from Figure 3.24 that the stress at break increases linearly with an increase in sisal content up to 30 % for the composites, which may be related to improved interfacial adhesion between the fibre and matrix. However, there is a decrease in the stress at break at higher sisal concentrations. Defects are formed at interfacial positions between the fibre and the matrix. Cracks, initiated at defect points, grow along the draw direction up to the sites with similar defects in the structure, when subjected to stress. This allows expansion of the cracks perpendicular to the draw direction. Since sisal fibre is dispersed within the continuous matrix of LLDPE, it may restrict the effective formation of a three-dimensional network. For this reason, the number of defects increases with an increase in sisal content. This will induce a decrease in the stress at break. The formation of a three-dimensional network, on the other hand, can prevent propagation of defects through the material. This is probably why there is an increase in stress at break for composites that are treated with 1 % DCP for a specific composite. The observation that stress at break values of the composite treated with 1 % DCP are higher than that of the pure matrix is in agreement with previous observations by Joseph *et al.* [36] on randomly oriented LDPE-sisal fibre composites. Cross-linking prevents the flow of molecules, and leads to lower crystallinity.



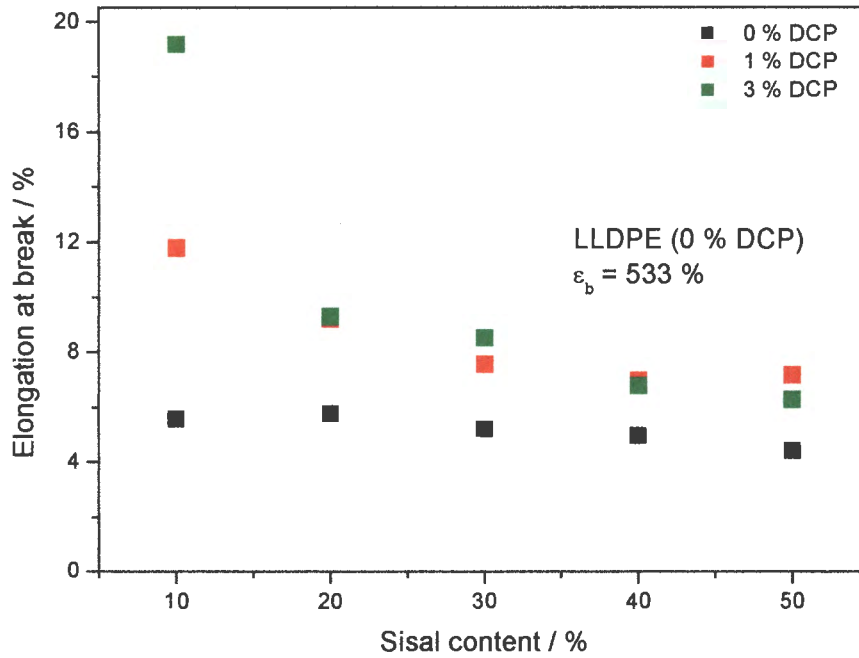


**Figure 3.22** Elongation at break as function of sisal content

**Table 3.7** Stress at break of LLDPE-sisal fibre composites

LL/D/S	$\sigma_b \pm s \sigma_b / \text{MPa}$	LL/D/S	$\sigma_b \pm s \sigma_b / \text{MPa}$	LL/D/S	$\sigma_b \pm s \sigma_b / \text{MPa}$
100/0/0	$11.4 \pm 0.1$	99/1/0	$11.8 \pm 0.1$	97/3/0	$12.4 \pm 1.3$
90/0/10	$8.0 \pm 0.2$	89/1/10	$11.1 \pm 0.0$	87/3/10	$16.5 \pm 3.9$
80/0/20	$11.1 \pm 0.4$	79/1/20	$15.1 \pm 0.2$	77/3/20	$19.5 \pm 2.1$
70/0/30	$14.2 \pm 0.5$	69/1/30	$17.2 \pm 0.1$	67/3/30	$18.8 \pm 1.2$
60/0/40	$12.1 \pm 3.0$	59/1/40	$17.7 \pm 0.2$	57/3/40	$21.7 \pm 2.8$
50/0/50	$11.3 \pm 1.0$	49/1/50	$17.2 \pm 1.7$	47/3/50	$17.4 \pm 1.4$

LL/D/S = mass percentage ratios of LLDPE/DCP/sisal

s = standard deviations

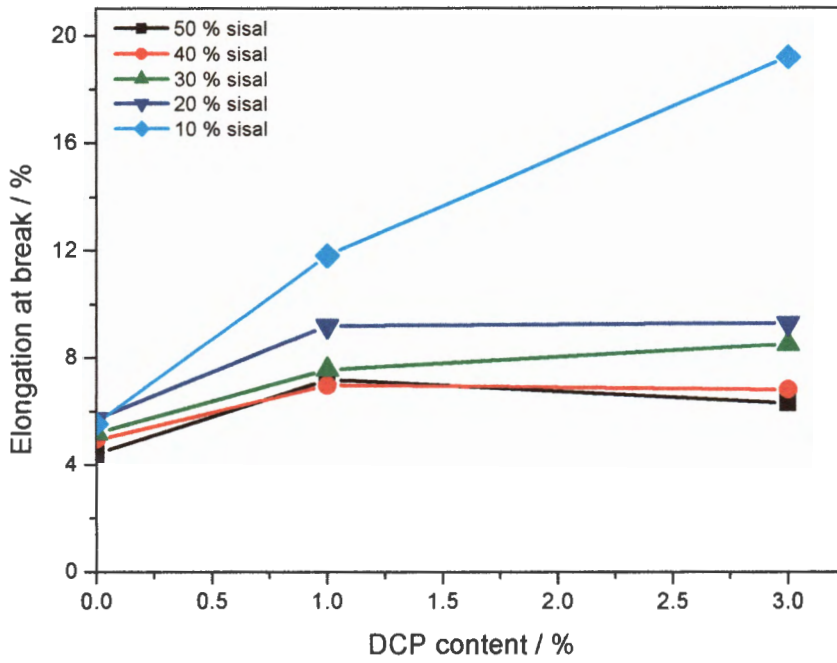


**Figure 3.23** Elongation at break as function of DCP content

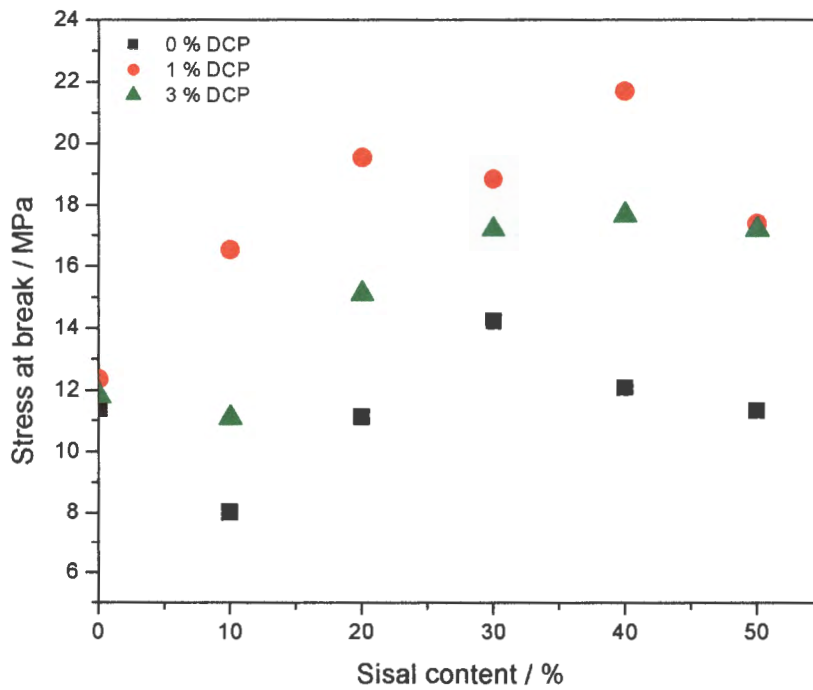


**Figure 3.24** Stress at break as function of sisal content

Figure 3.25 shows the effect of DCP on composites for different sisal content. The best results are obtained when 1 % DCP is used. That is, the stress at break seems to be higher for all sisal contents when the composites are prepared in the presence of 1 % DCP. The formation of a three-dimensional network increases the stress at break. The networks formed by cross-links absorb part of the mechanical energy necessary for pulling out the tie-chains. As a result a higher force is needed to break the material. High concentration of peroxide, however, introduces an enhanced number of defects in the material, which reduces the stress necessary to break it. As was mentioned earlier, defects are brought about by degradation caused by a too high DCP concentration.

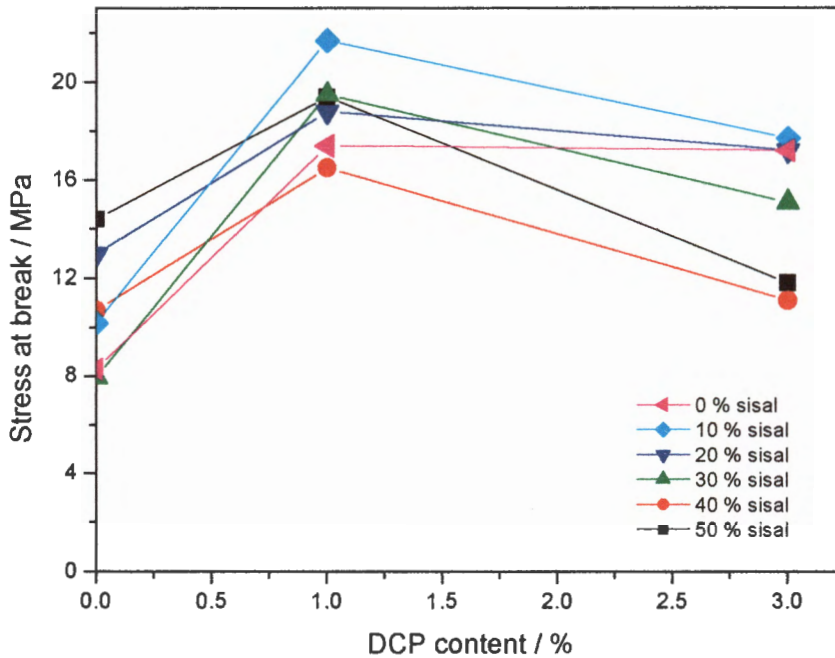


**Figure 3.25** Stress at break as function of DCP content

Table 3.8 gives a summary of the elastic modulus of pure LLDPE and its composites. The values increase with increasing sisal content (Figure 3.26). The values however, level off at high sisal contents. Composites that are treated with 1 % DCP show higher values than those treated with 3 % DCP, but generally DCP treatment does not have a substantial influence on the stiffness of the samples (Figure 3.27). Young's modulus increases with increasing sisal content because of the higher stiffness of sisal fibre. However, at high sisal contents the weak LLDPE-sisal fibre interface has a pronounced influence, and the modulus does not further increase. 1 % DCP treatment somehow improves LLDPE-sisal adhesion, leading to a stiffer composite. However, high DCP content brings about degradation of composites. This causes defects, which may lead to chain

scission and consequently brings about reduced mechanical properties. Another reason may be that a higher DCP content reduces the composites' crystallinity, which consequently lowers the elastic modulus of the composites. Elastic moduli generally increase with the amount of sisal for one specific DCP concentration. Introduction of the high modulus sisal fibres into the PE matrix enhances the modulus of the resulting material. Because of the relatively high stiffness of the fibre, the influence of the filler on the composite properties can roughly be explained in terms of the equal strain theory [38]. Assuming that loading produces equal strain in the matrix and the filler (of course, this is just as an approximation), the stress in the high modulus sisal fibres will be higher than in the matrix. Because of this, the fibre will take more of the strain energy, inducing an overall increase in the material modulus. This explains the increasing elasticity moduli with increasing sisal content. On the other hand, since the strain energy will be transferred from the matrix to the fibre, it is obvious that the matrix-fibre interaction is an important factor, which determines the final elastic properties of the composites. If there is grafting between LLDPE and sisal, as suggested by Joseph *et al.* [36], it will further contribute to an increase in elastic modulus. Mwaikambo *et al.* [38] also observed similar behaviour, where the stiffness or modulus of the untreated composites were increasing with an increase in fibre volume, and dropped slightly beyond about 23 % fibre volume fraction. This behaviour was attributed to an enhanced interfacial adhesion resulting from the presence of a matrix with increased polarity that may react or interact favourably with hydroxyl groups on the fibre surface.

**Table 3.8 Young's modulus of LLDPE-sisal fibre composites**

LL/D/S	E ± sE / MPa	LL/D/S	E ± sE / MPa	LL/D/S	E ± sE / MPa
100/0/0	151 ± 1	99/1/0	106 ± 11	97/3/0	74 ± 1
90/0/10	150 ± 10	89/1/10	194 ± 4	87/3/10	137 ± 5
80/0/20	233 ± 13	79/1/20	251 ± 6	77/3/20	174 ± 3
70/0/30	281 ± 35	69/1/30	261 ± 1	67/3/30	224 ± 7
60/0/40	243 ± 12	59/1/40	319 ± 20	57/3/40	300 ± 36
50/0/50	252 ± 13	49/1/50	292 ± 28	47/3/50	287 ± 7

LL/D/S = mass percentage ratios of LLDPE/DCP/sisal

s = standard deviations

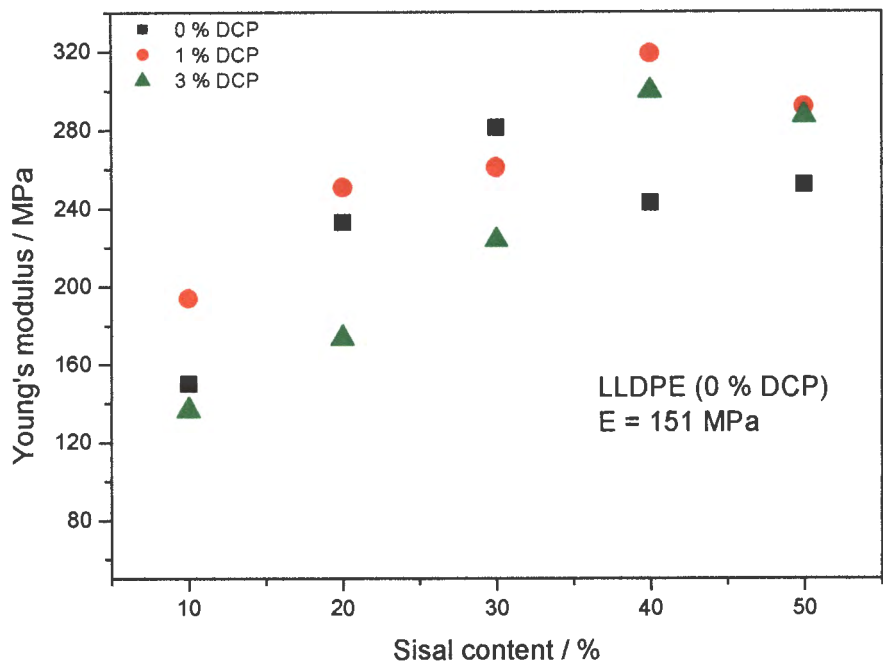


Figure 3.26 Young's modulus as function of sisal content

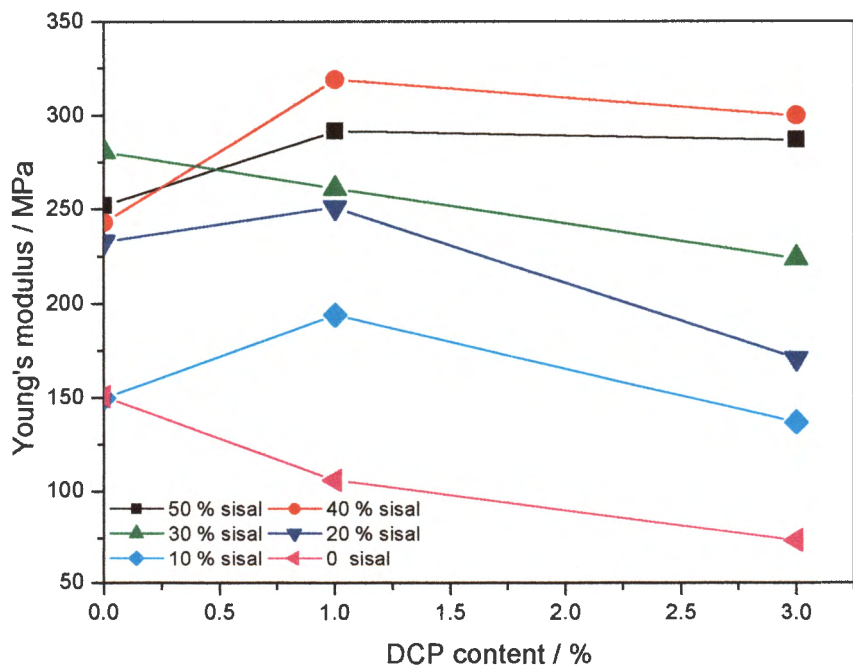


Figure 3.27 Young's modulus as function of DCP content



### 3.3.4 Stress relaxation

**Table 3.9 Stress relaxation of LLDPE-sisal composites**

LL/D/S	$\sigma / \sigma_0$	LL/D/S	$\sigma / \sigma_0$	LL/D/S	$\sigma / \sigma_0$
50/0/50	0.062	49/1/50	0.183	47/3/50	0.022
60/0/40	0.091	59/1/40	0.105	57/3/40	0.077
70/0/30	0.101	69/1/30	0.354	67/3/30	0.100
80/0/20	0.424	79/1/20	0.508	77/3/20	0.144
90/0/10	0.353	89/1/10	0.429	87/3/10	0.480
100/0/0	0.303	99/1/00	0.227	97/3/00	0.425

LL/D/S = mass percentage ratios of LLDPE/DCP/sisal

Stress relaxation curves as a function of time for untreated composites are represented in Figure 3.28. The curves are similar to typical relaxation curves of semi-crystalline polymers [42, 43] and polymer composites [34, 35] that were obtained in stress relaxation measurements in previous studies. In the beginning (up to 100 s) stress decaying is fast, but gradually slows down with time. The initial stresses depend in a similar way as modulus on the sisal content in the composites. In order to establish the effects of sisal content on the degree of stress decay, the relaxation curves in Figures 3.30 are normalized with respect to initial stress. The same was done to establish the effects of sisal content on 1 % DCP treated composites in Figures 3.29 and 3.31. Figure 3.32 shows the residual stresses after 90 min as function of sisal and DCP contents. There is a general increase in residual stress with increasing sisal content up to 30 % sisal for untreated composites, and for those treated with 1 % DCP. Above this concentration, however, the stress decreases. The 3 % DCP treated samples generally show residual stresses lower than the untreated and 1 % DCP treated samples. This observation is in contrary to that of Vanghese *et al.* [35], where the stress relaxation rate of composites of natural rubber reinforced with sisal fibre increases continually with an increase in sisal content. The difference in effect of sisal fibre on LLDPE and natural rubber may be attributed to the different relaxation mechanisms in these matrices.

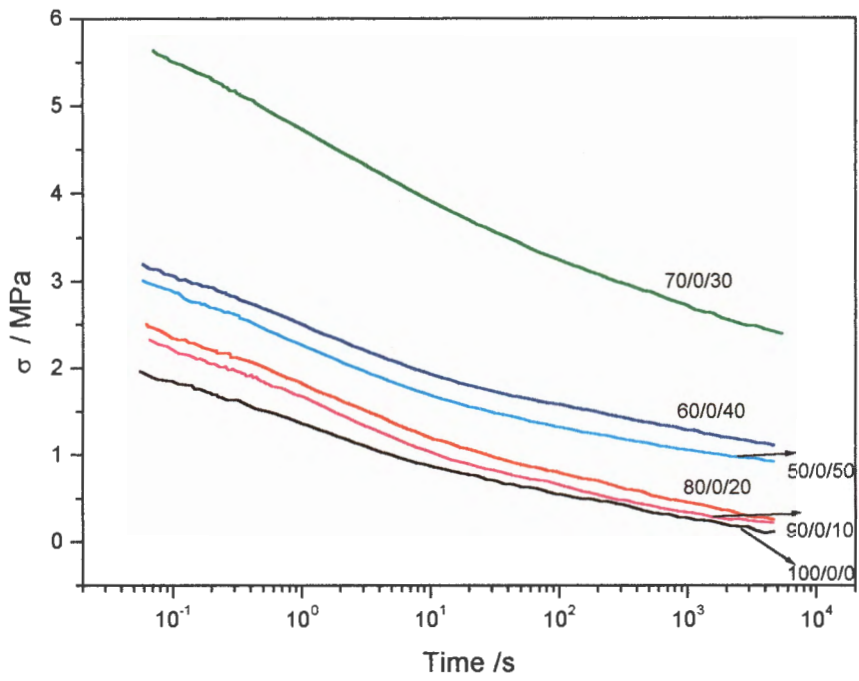


**Figure 3.28** Stress relaxation as function of time for untreated composites

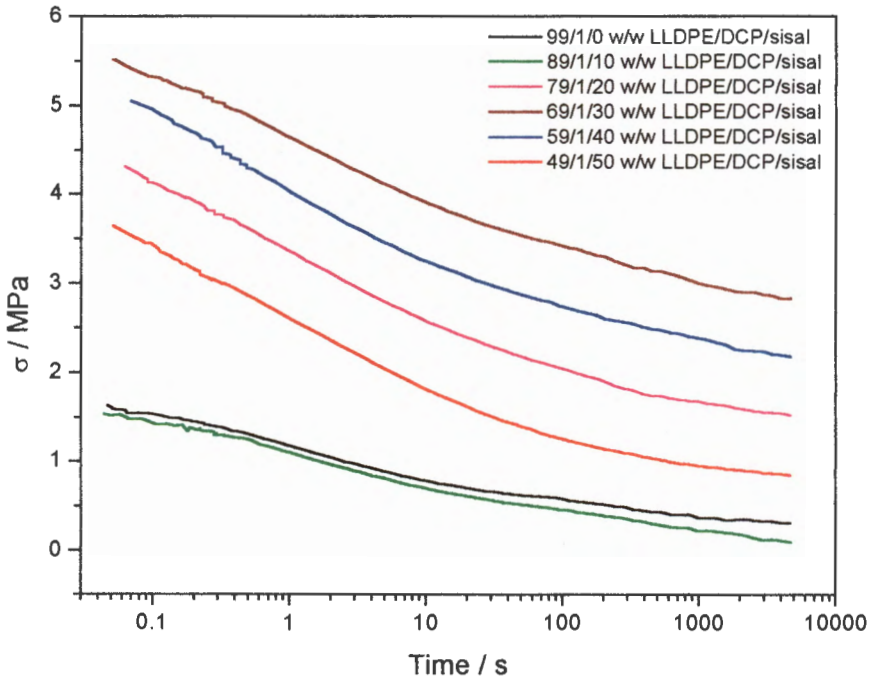


**Figure 3.29** Stress relaxation as function of time for 1% DCP treated composites

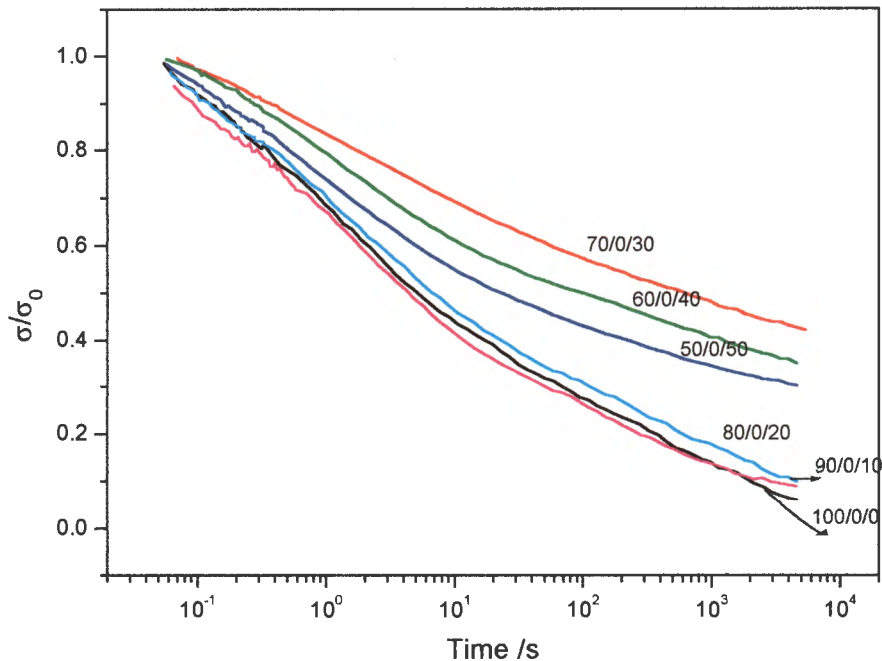


**Figure 3.30 Stress relaxation as function of time for untreated composites (normalized relative to initial stress relaxation)**

Stress relaxation in a semi-crystalline polymer, such as polyethylene, can be explained in terms of the two-process model [42, 43]. This model treats the stress relaxation in semi-crystalline polymers as a superposition of two thermally activated processes, each connected to one phase of the material, crystalline or amorphous. It is assumed that in the beginning of stress relaxation taut tie-chains that actually carry the applied load are pulled out from the crystal lamellae because they impose large local stresses. Taut tie-chains are, in fact, defects in the crystal structure at the points where they enter lamellae, and the stress concentration in these points is very high. Stress concentration induces defect propagation through the lamella, the so-called c-axis slip. As a consequence of this crystal process, the average distance between the lamellae increases until stretching of the formerly loose tie-chains takes place.

Since the applied stress is now re-distributed over a larger number of tie-chains, their propagation will be partially reduced and relaxation will start to slow down. This explains the presence of fast and slow relaxation processes in the experimental curves in Figure 3.28. In principle the above approach can also be applied to polymer composites if one treats the filler as “crystals” embedded in an amorphous matrix. However, instead of a crystal process or c-axis slip, a matrix filler debonding process should be considered. This can also be thought of in terms of the effect of thermal

motion on the orientation of polymer molecules. When a mechanical stress is applied to the composite, it introduces deformations of the chains. The entropy of the system decreases as less probable conformations are taken up. The free energy correspondingly increases. Because the composites are not elastic, they are kept in the deformed state. Stress relaxation takes place as a result of the thermal motion of the chains, the molecular deformations are obliterated, and the excess energy is dissipated as heat.

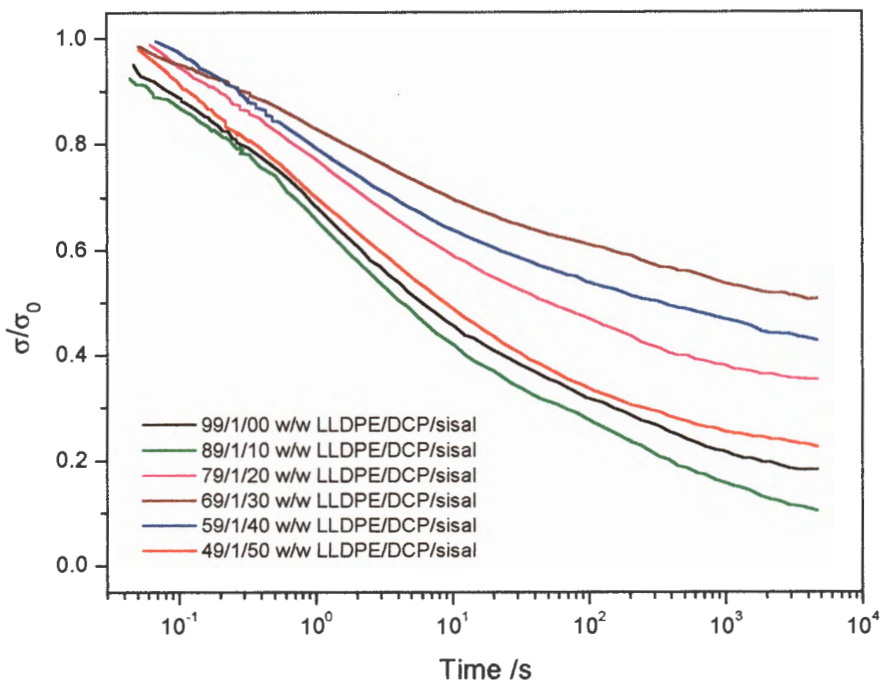


**Figure 3.31 Stress relaxation as function of time for composites treated with 1 % DCP (normalized relative to initial stress relaxation)**

The results on natural rubber-sisal fibre and natural rubber-carbon black composites could support the former conclusion [34, 35]. Pure rubber shows only one relaxation mechanism, whereas rubber composites show two distinguishable mechanisms. The crystallinity of a natural rubber is relatively low and the relaxation process takes place almost solely in the amorphous phase, which explains the presence of just one relaxation mechanism. A second, slow relaxation process arises after introduction of the filler through a progressive rubber-fibre de-bonding, similar to the slow releasing of the stress at lamellar defect points in a semi-crystalline polymer. Raman spectroscopy measurements by Van Eijk *et al.* [48] on polyethylene are also in line with the former discussion. They showed that, in the latter stage of relaxation, the number of high stress-bearing C-C bonds decreases with time in the same way as macroscopic stress. In the polyethylene-sisal fibre

composites the relaxation behaviour is more complicated because the crystal lamellae also contribute to the overall process. This could be the reason for the different effects of sisal fibre on the stress relaxation, as was mentioned above. It is possible that there is an interfacial load transfer to the filler and the total load is not only on the matrix, but is carried along by both the filler and the matrix. This may induce an increase in Young's modulus because the filler takes a lot of strain energy on itself. As long as the interaction between the filler and polyethylene chains is good i.e. while the modulus increases, this will stabilise the stress decay and the residual stress will also increase. At higher sisal loadings (40 and 50 %) the interaction between matrix and filler is relatively weak, which enables easier conformational rearrangements of PE-chains during stress relaxation. As a result, the stress decay will be more pronounced as shown in Figure 3.28.

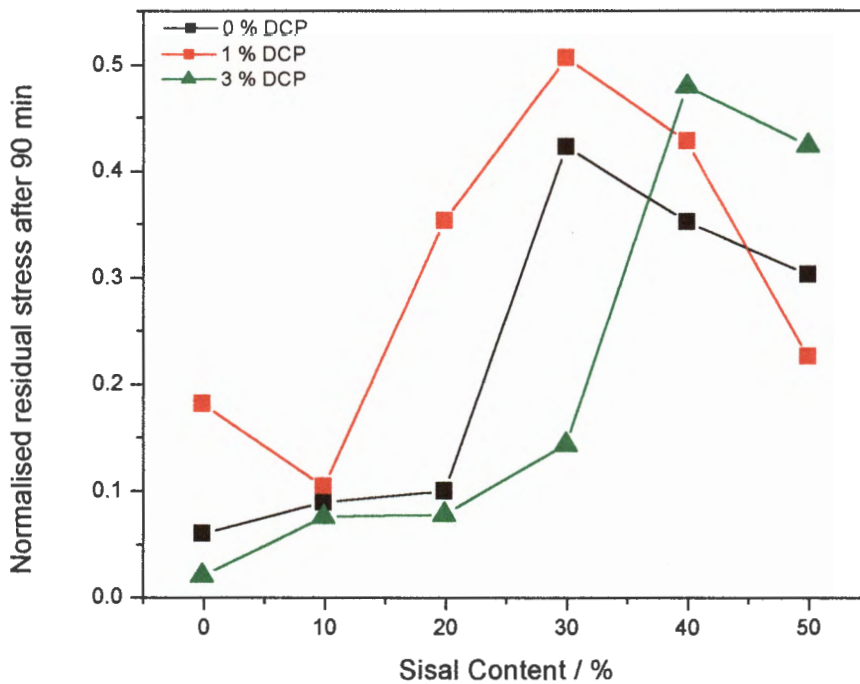


**Figure 3.32 Residual stress relaxation after 90 min as function of sisal content**

Figure 3.32 shows the changes in the visco-elastic properties with both sisal content and DCP concentration. Assuming that the application of stress leads to a de-bonding process between the matrix and filler, the results in this figure emphasises the importance of the strength of their interaction. It can be seen that composites melt pressed with 1 % DCP show higher values of normalised residual stress than the untreated composites, because of the improved interaction between the phases. The relaxation of the stress therefore depends on the viscosity coefficient of the material, which is inversely proportional to activation volume [47]. After fibre-matrix de-bonding,

the average activation volume of the chains increases, which reduces the viscosity and leads to a more intense cold flow. At low sisal contents (less than 30 %) the composite samples with 3 % DCP show lower values of residual stress than the untreated composite with the same amount of filler. The reason is probably degradation of the matrix at high peroxide concentrations. It is well known that the viscosity of the polymer decreases as its average molecular weight decreases. High concentrations (3 % DCP) will induce a large number of oxidative chain scissions, besides cross-linking, which will reduce the viscosity and consequently the residual stress. However, when the sisal content exceeds 30 %, grafting effects may start to override the effects of scission.

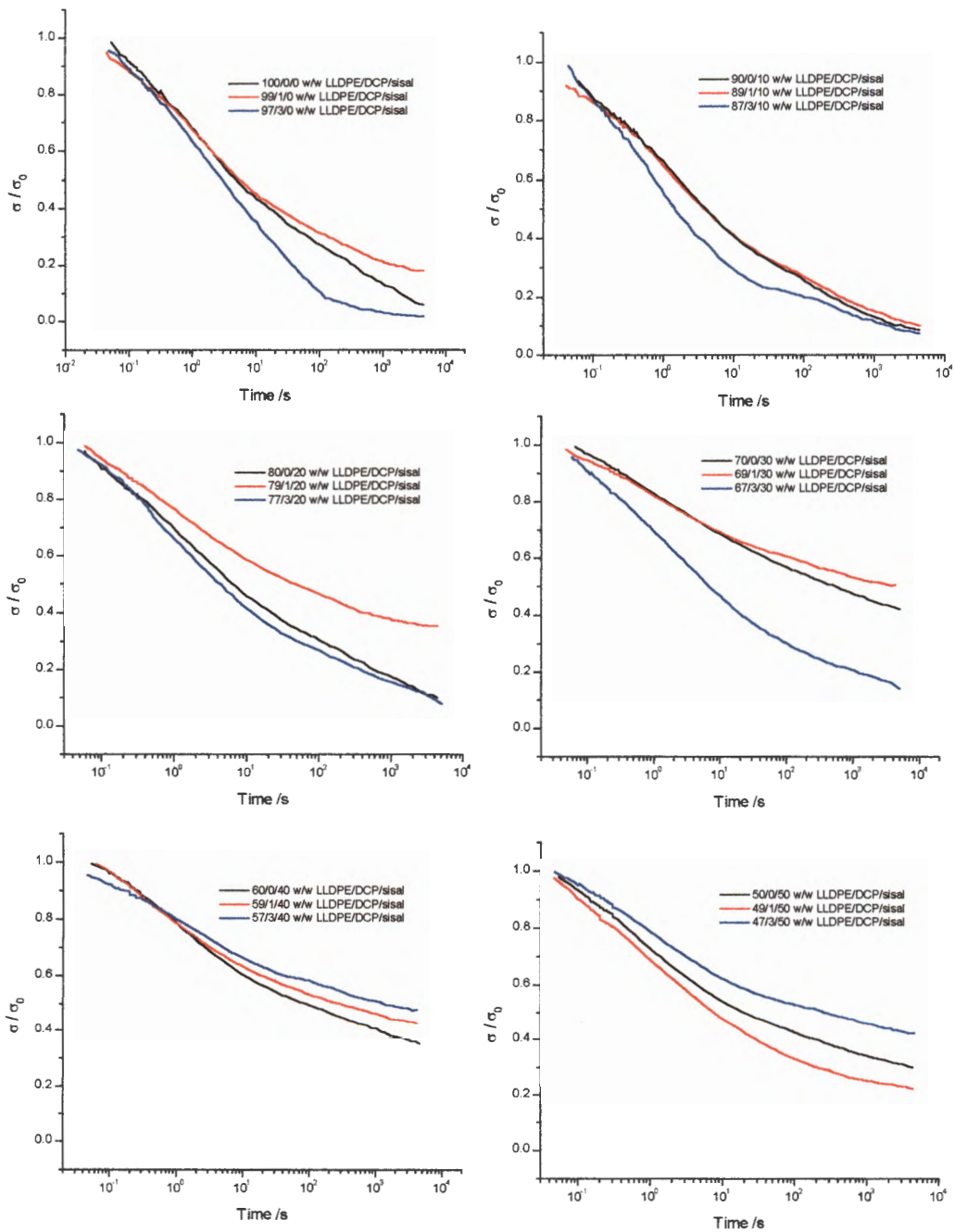


**Figure 3.33** Stress relaxation as function of time (normalized to initial stress relaxation)

Figure 3.33 shows the stress relaxation behavioural patterns of all the composites as a function of time. It should be noted that the composites treated with DCP show similar relaxation behaviour as the untreated ones. The normalised residual stresses show small changes in initial stresses with sisal content for one specific DCP concentration. An increase in the normalised residual stresses implies an improved stability of the material upon prolonged loading.

### 3.5 Microscopy

Figures 3.34 to 3.35 show optical microscopic photographs of the LLDPE-sisal fibre composites. From these figures it can be seen that the fibres are separated and have a diameter of approximately 57  $\mu\text{m}$ . It can also be seen in Figure 3.34 that the surfaces of the fibres in the composites, treated with DCP, appear smoother than in the untreated ones. There is also a reduction in the thickness of the fibre upon treatment of composites with DCP. This may be due to the leaching out of moisture and possibly other fractions of fibre during treatment with DCP. The treatment also produces a number of small voids on the surface of the fibre that may promote mechanical interlocking between the fibre and the matrix [8, 9]. It is further important to note that reduction of fibre diameter is more pronounced for composites that are treated with 1 % DCP at small fibre loading compared to their 3 % counterparts. The pictures also indicate inhomogeneous distribution of the short fibre in the LLDPE matrix, which may be the reason for the scatter in enthalpy values obtained during thermal analysis.

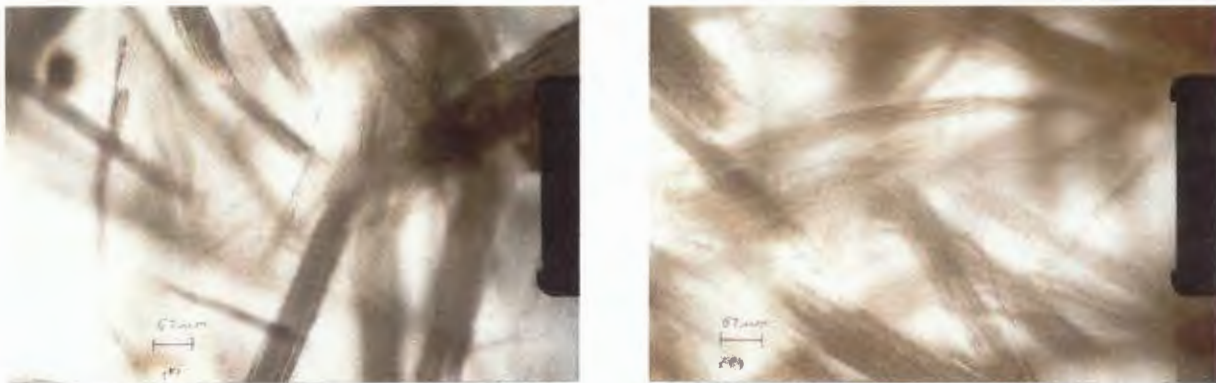


**Figure 3.34 Optical microscopy photos of pure sisal fibre (left) and 89/1/20 w/w LLDPE/DCP/sisal (right)**



**Figure 3.35** Optical microscopy photos of 77/3/20 (left) and 79/1/20 w/w LLDPE/DCP/sisal (right)



**Figure 3.36** Optical microscopy photo of 87/3/20 LLDPE/DCP/sisal



## CHAPTER 4

### CONCLUSIONS

Having realised that sisal fibre, which is easily attainable in South Africa, has good mechanical properties, it was assumed that it could be used as a filler to strengthen LLDPE composites. The effect of sisal fibre on the mechanical and thermal properties of untreated and treated sisal fibre reinforced LLDPE composites were, therefore, investigated. The inherent difficulty is that sisal is hydrophilic (high rate of water absorption), while LLDPE is hydrophobic. This gives poor sisal-polymer interfaces in the composite. I therefore decided to treat the composites with DCP to improve interfacial adhesion in the fibre-reinforced polymer composites. The objective of this study was to investigate the influence of differing contents of DCP and sisal fibre on the properties of LLDPE-sisal fibre composites.

The characterisation of the LLDPE-sisal composites by using gel content measurements and FTIR spectra has proved difficult in this work. However, the gel content measurement showed a slight decrease in extent of cross-linking with an increase in the sisal fibre content in the case of 1 % DCP treated composites. The gel content remained constant with increasing sisal content when 3 % DCP was used. FTIR spectra showed a significant reduction in the OH vibration absorption at  $3340\text{ cm}^{-1}$  in the composites treated with DCP. This may be the result of grafting between LLDPE and sisal and/or reduced moisture uptake by the composites.

The composites absorb water in proportion to the amount of sisal it contains. Measurement of the water absorption shows that DCP treatment improves the composites' absorption properties, but degradation plays a role when a higher amount of DCP is used. The reduced water absorption is probably the result of improved interfacial adhesion resulting from cross-linking of the LLDPE matrix and/or grafting between LLDPE and sisal.

The softening point of treated polymer composites increases with increasing sisal fibre content. The values for 1 % and 3 % DCP treated samples does not differ much, but in the case of 3 % DCP treated samples with high fibre content, no softening points were observed within the investigated temperature range.

All the composites showed only one peak for both the DSC heating and cooling curves, which suggests that only LLDPE melts in this temperature range. In the case of untreated composites the

melting temperatures do not change significantly with increasing sisal content, which indicates that under these circumstances sisal does not have a remarkable influence on the LLDPE crystalline morphology. Cross-linking and/or grafting, however, leads to lower melting temperatures, that further decrease with increasing sisal content. This clearly indicates a changed crystalline structure, which includes thinner lamellae. The enthalpies, and therefore crystallinities, also decrease for DCP treated samples.

Peroxide treatment can improve the ultimate tensile properties of the composites, especially when a small quantity is used. The addition of a low concentration of 1 % DCP in the composites of LLDPE and short sisal fibres, prepared by mechanical mixing and subsequent melt pressing, significantly improves tensile and visco-elastic properties. Composite samples with 1 % DCP have a significantly higher strength and elastic modulus than the untreated ones with the same amount of filler. Consequently cross-links and/or grafts improve their, otherwise, poor adhesion. Formation of a three-dimensional network prevents defect propagation, and the stress concentration leads to an increase in both stress and strain at break. Higher content of DCP and sisal fibre, however, shows detrimental effect on the mechanical properties of composites.

Stress decaying of composites is fast but gradually slows down with time. Stress relaxation measurements showed that cross-linking and/or grafting reduces the degree of permanent deformation of the composites while they are kept for longer times under constant strain. The residual stress relaxations after 90 min show a gradual increase at low sisal contents, but this decreases drastically at high sisal fibre contents. This shows that reinforcement of LLDPE was a success. As the composite is subjected to stress, not only the matrix takes the strain, but there is also an interfacial load transfer to the filler, so that both the filler and matrix carry the stress. However, high DCP concentration induces degradation of the matrix at low sisal contents (< 30 %). This is why these samples are less stable upon prolonged loadings compared to their untreated counterparts. Composites in which 1 % DCP was used, showed higher values of residual stress than the untreated composites. This strongly supports improved LLDPE-sisal fibre interfacial adhesion. Stress relaxation measurements also suggest reduction in the viscosity of the composites, which leads to a more intense cold flow.

Optical microscopic photographs showed no homogeneity of the fibre within the matrix. The addition of DCP in the composites produces smoother fibres and reduction in diameter. This was an indication that moisture is reduced as DCP is used to treat the composites. It was, however, shown that composites treated with 1 % DCP showed smoother fibres than those treated with 3 %

DCP for the same fibre loading. The treated composites gave stronger interfacial adhesion to the polymer than the untreated composites.

### *Future prospects*

Over the past decade, cellulosic fillers of have been and continue to be of great interest, as they give composites with improved mechanical properties compared to those containing non-fibrous fillers. Studies showed that lingo-cellulosic fibres like jute, sisal, coir and pineapple have been used as reinforcement in thermoset and thermoplastic materials. Among these fibres, sisal proved to be of particular interest in that its composites have high impact strength besides having moderate tensile and flexural properties compared to other ligno-cellulosic fibres. Other investigations, including this study, highlight that sisal fibre can also be used as reinforcement in a thermoplastic matrix and it performs better than wood fibres [31]. Another motivating factor regarding the continuity of this study is the cost factor: sisal fibre is produced in abundance in South Africa and is thus easily accessed. It is also important to mention that sisal fibre does not pose any health hazard to ones' health since it contains no toxic components.

This study reveals many interesting observations on the physical properties of both untreated and DCP treated LLDPE-sisal fibre composites. Observed improvements are due to possible enhanced interfacial adhesion between the matrix and the fibre. For future studies sisal fibre will be used as long fibre and other types of treatments will also be investigated. Different types of matrix like PP or epoxy resin, might be investigated. Other techniques such as injection moulding or laminating will be implemented.

The effect of water absorption on thermal and mechanical properties of composites reinforced with sisal fibre may prove interesting for future studies. The homogeneity of fibre within the matrix may be improved by melt-mixing the samples in a Brabender melt-mixer or extruder. From this study, it was shown that DCP treated or modified sisal fibre reinforced composites are potential structural materials, as a result of their improved mechanical and environmental properties as well as economic factors. It is however, necessary to consider an extended study on the material in order to further create a range of technological applications beyond its traditional use as ropes, carpets mats, etc. Economical processing methods must be developed for the composites and the relationship between the mechanical properties and processing methods should be established. Microstructure of the interface between sisal fibre and matrix still needs to be investigated.

## REFERENCES

1. Al-Malaika S, *Reactive Modifiers for Polymers*, Blackie Academic and Professional, London (1997)
2. Felix JM and Gatenholm P, *Journal of Materials Science*, **29**, 3043-3049 (1994)
3. Bledzki AK and Gassan J, *Progress in Polymer Science*, **24**, 221-274 (1999)
4. Van de Velde K and Kiekens P, *Polymer Testing*, **20**, 885-893 (2001)
5. Li Y, Yiu-Wing M and Lin Y, *Composite Science and Technology*, **60**, 2037-2055 (2000)
6. Gangopadhyay R and Ghosh P, *European Polymer Journal*, **36**, 1597-1606 (2000)
7. Edwards HGM, Farwell DW and Webster D, *Spectrochimica Acta Part A*, **53**, 2383-2392 (1997)
8. Khalil HPSA, Ismail H, Rozman HD and Ahmad MN, *European Polymer Journal*, **37**, 1037-1045 (2001)
9. Albano C, Gonzalez J, Ichazo M and Kaiser D, *Polymer Degradation and Stability*, **66**, 179-190 (1999)
10. Baiardo M, Frisoni G, Scandola M and Licciardello A, *Journal of Applied Polymer Science*, **83**, 38-45 (2002)
11. Billmeyer Jr FW, *Textbook of Polymer Science*, John Willey and Sons Inc., London (1984)
12. Colin B and Colin P, *Comprehensive Polymer Science*, **2**, Pergamon Press, Frankfurt (1989)
13. Orchard GAJ, Davies GR and Ward IM, *Polymer*, **25**, 1203-1210 (1984)
14. Smith WF, *Principles of Materials Science and Engineering*, 2<sup>nd</sup> edition, McGraw-Hill, London (1990)
15. Hlangothi S P, Krupa I, Djoković V and Luyt A S, *Polymer Degradation and Stability*, **79**, 53-59 (2003)
16. Vasile C and Kulshreshtha AK, *Handbook of Polymer Blends and Composites*, **3**, Rapra Technology Limited, United Kingdom, (2003)
17. Krupa I and Luyt A S, *Journal of Applied Polymer Science*, **81**, 973-980 (2001)
18. Turcsanyi B, Pukanszky B and Tudos F, *Journal of Materials Science*, **7**, 160-162 (1988)
19. Hunt BJ and James MI, *Polymer Characterisation*, Blackie Academic & Professional, New York (1997)
20. Filho TRD and Sanuan MA, *Cement and Concrete Research*, **29**, 1597-1604 (1999)
21. Zadorecki P and Michell AJ, *Polymer Composites*, **10**, 69-77 (1989)
22. Balasuriya PW, Ye L and Mai YW, *Composites: Part A*, **32**, 619-629 (2001)
23. Privalko EG, Pedosenko AV, Privalko VP, Walter R and Friedrich K, *Journal of Applied Polymer Science*, **73**, 1267-1271 (1999)

24. Amash A and Zugenmaier P, *Polymer*, **41**, 1589-1596 (1999)
25. Amash A and Zugenmaier P, *Journal of Applied Polymer Science*, **63**, 1143-1154 (1997)
26. Raghavan D and Emekalam A, *Polymer Degradation and Stability*, **72**, 509-517 (2001)
27. Kalaprasad G, Pradeep P, Mathew G, Pavithran C, and Thomas S, *Composites Science and Technology*, **60**, 2967-2977 (2000)
28. Zang YH and Sapeiha S, *Polymer*, **32**, 489-492 (1991)
29. Mishra S, Naik JB and Patil YP, *Composites Science and Technology*, **60**, 1729-1735 (2000)
30. Danjaji ID, Nawang R, Ishiaku US and Mohd Ishak ZAM, *Polymer Testing*, **21**, 75-81 (2002)
31. D'Almeida JRM and De Carvalho LH, *Journal of Material Science*, **33**, 2215-2219 (1998)
32. Pukanszky B, *Composites*, **21**, 255-262 (1990)
33. Felix JM and Gatenholm P, *Journal of Applied Polymer Science*, **50**, 699-708 (1993)
34. MacKenzie CI and Scanlan J, *Polymer*, **25**, 559-568 (1984)
35. Varghese S, Kuriakose B and Thomas S, *Journal of Applied Polymer Science*, **53**, 1051-1060 (1994)
36. Joseph K, Thomas S and Pavithran C, *Polymer*, **37**, 5139-5149 (1996)
37. Joseph K, Thomas S and Pavithran C, *Composites Science and Technology*, **53**, 99-110 (1995)
38. Mwaikambo LY, Martuscelli E and Avella M, *Polymer Testing*, **19**, 905-918 (2000)
39. Li Y, Fan Yunge and Ma J, *Polymer Degradation and Stability*, **73**, 163-167, (2001)
40. Bershtein VA and Egorov MV, *Polymer Science and Technology*, McGraw-Hill, London (1994)
41. Mark A, *Polymer Science Dictionary*, 2<sup>nd</sup> edition, Chapman and Hall, New York (1997)
42. Djoković V, D Kostoski D, Dramićanin MD and Suljovrujić E, *Polymer Journal*, **31**, 1194 (1999)
43. Djoković V, D Kostoski D and Dramićanin MD, *J. Polymer Science Part B Polym. Phys.* **38**, 3239 (2000)
44. Joseph K, Thomas S and Pavithran C and Brahmakumar M, *Journal of Applied Science*, **47**, 1731 (1993)
45. Stael GC, Tavares MIB and d'Almeida JRM, *Polymer Testing*, **20**, 869 (2001)
46. Prasantha KR, Manikadan Nair KC, Thomas S, Schit SC and Ramamurrthy K, *Composite Science and Technology*, **60**, 1737 (2000)
47. Jennes JR and Kline DE, *Journal of Applied Polymer Science*, **17**, 3391 (1973)
48. Van Eijk MCP, Leblans PJR, Meier RJ and Kip BJ, *Journal of Material Science Letters*, **9**, 1263 (1990)

49. Doolittle AK and Doolittle DB, *Journal of Applied Physics*, **28**, 901 (1957)
50. Gan D, Lu S, Song C, Wang Z, *European Polymer Journal*, **37**, 1359-1365 (2001)
51. Rajeev K, Mohan K and Ramani N, *Polymer Engineering and Science*, **37**, 446-483, (1997)
52. Manikandan Nair KC, Thomas S, and Groeninckx, *Composites Science and Technology*, **61**, 2519-2529, (2001)
53. Krupa I and Luyt AS, *Journal of Applied Polymer Science*, **81**, 973-980 (2001)
54. Rana SK, *Journal of Applied Polymer Science*, **83**, 2604-2608 (2002)
55. Luo X, Benson RS, Kit KM and Dever M, *Journal of Applied Polymer Science*, **85**, 1961-1969 (2002)
56. Nicholson JW, *The Chemistry of Polymers*, Royal Society of Chemistry, London (1991)
57. Chant N and Tiwary RK, *Journal of Materials Science*, **23**, 381-387 (1998)

